

1 **Genome-Wide Identification and Characterization of *Fusarium circinatum*-**
2 **Responsive lncRNAs in *Pinus radiata***

3 Zamora-Ballesteros, C.^{1,2}; Martín-García, J.^{1,2}; Suárez-Vega, A.³; Diez, J.J.^{1,2}

4 ¹ Sustainable Forest Management Research Institute, University of Valladolid—INIA,
5 Palencia, 34004, Spain

6 ² Department of Vegetal Production and Forest Resources, University of Valladolid,
7 Palencia, 34004, Spain

8 ³ Department of Animal Production, Faculty of Veterinary Medicine, University of
9 León, Campus de Vegazana s/n, León, 24071, Spain

10 One of the most promising strategies of Pine Pitch Canker (PPC) management is the use
11 of reproductive plant material resistant to the disease. Understanding the complexity of
12 plant transcriptome that underlies the defence to the causal agent *Fusarium circinatum*,
13 would greatly facilitate the development of an accurate breeding program. Long non-
14 coding RNAs (lncRNAs) are emerging as important transcriptional regulators under
15 biotic stresses in plants. However, to date, characterization of lncRNAs in conifer trees
16 has not been reported. In this study, transcriptomic identification of lncRNAs was
17 carried out using strand-specific paired-end RNA sequencing, from *Pinus radiata*
18 samples inoculated with *F. circinatum* at an early stage of infection. Overall, 13,312
19 lncRNAs were predicted through a bioinformatics approach, including long intergenic
20 non-coding RNAs (92.3%), antisense lncRNAs (3.3%) and intronic lncRNAs (2.9%).
21 Compared with protein-coding RNAs, pine lncRNAs are shorter, have lower
22 expression, lower GC content and harbour fewer and shorter exons. A total of 164
23 differentially expressed (DE) lncRNAs were identified in response to *F. circinatum*

1 infection in the inoculated versus mock-inoculated *P. radiata* seedlings. The predicted
2 *cis*-regulated target genes of these pathogen-responsive lncRNAs were related to
3 defence mechanisms such as kinase activity, phytohormone regulation, and cell wall
4 reinforcement. Co-expression network analysis of DE lncRNAs, DE protein-coding
5 RNAs and lncRNA target genes also indicated a potential network regulating
6 pectinesterase activity and cell wall remodelling. This study presents the first analysis of
7 conifer lncRNAs involved in the regulation of defence network and provides the basis
8 for future functional characterizations of lncRNAs in relation to pine defence responses
9 against *F. circinatum*.

10 **1. Introduction**

11 The major portion (98-99 %) of the transcribed genome comprises genetically inactive
12 material known as non-coding RNA (ncRNA) (Lozada-Chávez *et al.* 2011). Among the
13 ncRNA, the well-known housekeeping RNAs (transfer and ribosomal RNA) or small
14 regulatory molecules including microRNAs (miRNAs), small nuclear RNAs (snRNAs)
15 and small silencing RNAs (siRNAs) can be found (Bonnet *et al.* 2006). During the last
16 decade, an heterogeneous class of ncRNA, long non-coding RNA (lncRNA), has
17 emerged as another eukaryotic non-coding transcript class that had been largely ignored
18 by molecular biologists (Tripathi *et al.* 2017). However, accumulating evidence
19 supports that lncRNAs participate in many cellular processes by regulating gene
20 expression in different manners (Quan *et al.* 2015). In this new and heterogeneous class,
21 all transcripts greater than 200 nt in length that lack coding potential are included
22 (Kapranov *et al.* 2007). Similar to protein-coding genes, lncRNAs are transcribed by
23 RNA polymerase II, capped, polyadenylated and usually spliced (Quan *et al.* 2015).
24 Some lncRNAs, termed *cis*-acting lncRNAs, regulate molecular processes around their

1 transcription site, whereas *trans*-acting lncRNAs leave their transcription sites to exert
2 their function elsewhere (Gil and Ulitsky 2020). LncRNAs are usually further sub-
3 divided according to their function or based on their location and orientation with
4 respect to the nearest protein-coding gene in the genome (Rai *et al.* 2019). Sense and
5 anti-sense, intergenic as well as intronic (located into an intron) are the main groups for
6 classifying the lncRNAs according to their genomic location (Ma *et al.* 2013). On the
7 other hand, the reported functions for this class of transcripts differ substantially.
8 Known mechanism of action including molecular signalling, decoys (binding to
9 regulatory elements such as miRNAs blocking their molecular interaction), guides
10 (directing specific RNA-protein complexes to specific targets) and scaffolds as central
11 platforms for regulation, are associated to the majority of lncRNAs (Wang and Chang
12 2011).

13 The growing number of studies focusing on the interference of plant lncRNAs in
14 different biological processes, including fertility, photomorphogenesis, wood formation,
15 and biotic and abiotic stress, has demonstrated their important regulatory role in the
16 transcription system (Chen *et al.* 2015; Liu *et al.* 2015; Sanchita *et al.* 2020). Some of
17 these lncRNAs have been experimentally validated, most of them being from model
18 plants. For example in *Arabidopsis*, two lncRNAs, COOLAIR and COLDAIR, have
19 been shown to be crucial in the regulation of cold stress response (Swiezewski *et al.*
20 2009; Heo and Sung 2011). Likewise, DRIR lncRNA regulates the expression of a
21 series of genes involved in drought and salt stress-responsive (Qin *et al.* 2017). The
22 regulatory role of the lncRNA IPS1 has also been reported blocking the miRNA mir399
23 that suppress the expression of the gene responsible for the phosphate uptake (Franco-
24 Zorrilla *et al.* 2007). Moreover, some lncRNAs associated with biotic stress have been
25 characterized in plants. These included lncRNAs that regulate positively the expression

1 of defence-related PR genes such as ELENA1, identified in *Arabidopsis* as a factor
2 enhancing resistance against the pathogen *Pseudomonas syringae*, and lncRNA39026
3 that increases resistance against *Phytophthora infestans* in tomato (Seo *et al.* 2017; Hou
4 *et al.* 2020). The biosynthesis or signalling of plant hormones have been altered by
5 lncRNAs as well. In cotton plants, the silencing of two lncRNAs (GhlncNAT- ANX2
6 and GhlncNAT-RLP7) led to increased resistance to *Verticillium dahliae* and *Botrytis*
7 *cinerea*, possibly due to the transcriptional induction of two lipoxygenases involved in
8 the jasmonic acid defence signalling pathway (Zhang *et al.* 2018). In addition,
9 overexpression of lncRNA ALEX1 in rice increased jasmonic acid levels enhancing
10 resistance to the bacteria *Xanthomonas oryzae* pv. *oryzae* (Yu *et al.* 2020).

11 Next Generation Sequencing (NGS) technologies and computational methods have
12 enabled a deeper study of the transcriptomic data and have been widely applied for the
13 identification and characterization of plant lncRNAs (Tripathi *et al.* 2017). Recently, a
14 number of lncRNAs involved in plant-pathogen interactions has been computationally
15 predicted in non-model plants. In *Brassica napus*, 931 lncRNAs were identified in
16 response to *Sclerotinia sclerotiorum* infection, one of them (TCONS_00000966) as
17 antisense regulator of genes involved in plant defence (Joshi *et al.* 2016). Li *et al.*
18 (2017) discovered *Musa acuminata* lncRNAs related to resistance against *Fusarium*
19 *oxysporum* f. sp. *cubense* infection. Particularly, lncRNAs involved in the expression of
20 pathogenesis-related proteins and peroxidases were mainly induced in the resistant
21 cultivar, whereas lncRNAs related to auxin and salicylic acid signal transductions could
22 predominantly be induced in the susceptible cultivar. In the Paulownia witches' broom
23 disease interaction, nine lncRNAs were predicted to target twelve genes based on a co-
24 expression network model in the tree (Wang *et al.* 2017). In kiwifruit leaves infected by
25 *P. syringae*, a weighted gene co-expression network analysis revealed a number of

1 lncRNAs closely related to plant immune response and signal transduction (Wang *et al.*
2 2017). Likewise, Feng *et al.* (2021) identified 14,525 lncRNAs related to the walnut
3 anthracnose resistance. This analysis showed that the target genes of the up-regulated
4 lncRNAs were enriched in immune-related processes during the infection of the causal
5 agent *Colletotrichum gloeosporioides*. These studies highlight the important role of
6 lncRNAs in plant defence, thus further research is needed to decipher their function and
7 interference in the transcriptomic system.

8 *Fusarium circinatum* is an invasive pathogen that causes the Pine Pitch Canker (PPC).
9 This disease affects conifers, resulting in a serious economic and ecological impact on
10 nurseries and pine stands (Wingfield *et al.* 2008). Since the first report in 1946 in North
11 America, the presence of *F. circinatum* has been notified in 14 countries of America,
12 Asia, Africa and Europe (Drenkhan *et al.* 2020). The long-distance dispersion as a result
13 of globalization of plant trade and movement of contaminated soil and seed, represents
14 the main pathway for new introductions of the pathogen into disease-free regions
15 (Zamora-Ballesteros *et al.* 2019). The establishment of the disease in field is of great
16 concern since no feasible measures are available to control or eradicate *F. circinatum*
17 (Martín-García *et al.* 2019). Thus, the development of resistant genotypes through
18 breeding and/or genetic engineering may be one of the most efficient PPC management
19 strategy in the long-term (Gordon *et al.* 2015; Martín-García *et al.* 2019). In this
20 context, several transcriptome analyses with the aim of unravelling molecular defence
21 responses have provided detailed insights about the molecular mechanisms underlying
22 disease progression in the *Pinus-F. circinatum* pathosystem. These studies have
23 examined the response of hosts through a different degree of susceptibility, from highly
24 susceptible (*Pinus radiata*, *Pinus patula*) to moderate (*Pinus pinaster*) and highly
25 resistant (*Pinus tecunumanii*, *Pinus pinea*) (Visser *et al.* 2015, 2018, 2019; Carrasco *et*

1 *al.* 2017; Hernandez-Escribano *et al.* 2020; Zamora-Ballesteros *et al.* 2021). However,
2 the role of lncRNAs in the regulation of defence network in conifers has not been
3 studied yet. In the present study, a strand-specific RNA-Seq has been conducted in
4 order to characterize lncRNAs present in high susceptible *P. radiata* and elucidate how
5 lncRNA expression profiles change in response to *F. circinatum* infection.

6 **2. Material and methods**

7 2.1. Inoculum preparation and inoculation trial

8 The *F. circinatum* isolate 072 obtained from an infected *P. radiata* tree in the North of
9 Spain (Cantabria, Spain) was used. The isolate was cultured in Petri dishes containing
10 PDA medium (Scharlab S.L., Spain) for a week at 25 °C. Then, to stimulate the
11 sporulation of the fungus, four mycelial agar plugs were subcultured in an Erlenmeyer
12 flask with 100 mL of PDB medium (Scharlab S.L., Spain) and incubated in an orbital
13 shaker at 150 rpm during 48 hours at 25°C. Afterwards, the conidial suspension was
14 adjusted with a haemocytometer at 10^6 conidia mL⁻¹ for the inoculation.

15 Six-month-old seedlings of *P. radiata* (Provenance: Galicia, Spain) with an
16 approximate stem diameter of 2.5 ± 0.5 cm were inoculated on the stem by making a
17 wound with a sterile scalpel and pipetting 10 µL of conidial suspension (Martin-Garcia
18 *et al.* 2017). The same process was applied for the control seedlings that were mock-
19 inoculated with sterilized distilled water. The inoculated wound was immediately sealed
20 with Parafilm® to prevent drying. Sixty seedlings were inoculated for each treatment
21 (inoculation with pathogen and mock-inoculation). Plants were placed in a growth
22 chamber at 21.5 °C with a 14-h photoperiod and kept for 67 days during which mortality
23 rates were daily recorded.

1 The survival analysis based on the non-parametric estimator Kaplan-Meier (Kaplan and
2 Meier 1958) was performed with the “Survival” package (Therneau 2020) to test the
3 mortality of the plants. Survival curves were created with the “Survfit” function and the
4 differences between the curves were tested with the “Survdiff” function. All analyses
5 were performed using R software environment (R Core Team 2019).

6 2.2. RNA extraction and paired-end strand-specific sequencing

7 A piece of the stem from the upper part of the inoculation point (*ca.* 1 cm length) was
8 sampled at four days post-inoculation (dpi) for the transcriptomic analysis. The
9 harvested tissues were immediately frozen in liquid nitrogen and ground to a fine
10 powder using a mortar and pestle. RNA extraction were performed using the
11 Spectrum™ Plant Total RNA Kit (Sigma Aldrich, USA) following the manufacturer’s
12 protocols including the optional on-column DNase 1 digestion (DNASE10-1SET,
13 Sigma-Aldrich, St. Louis, MO, USA). After RNA extraction, samples were transferred
14 to RNase- and DNase-free tubes (Axygen®, USA) and stored at -80 °C. The
15 concentration and purity of the RNA extracted were measured using the Multiskan GO
16 Spectrophotometer ($A_{260}/A_{280} \geq 1.8$, $A_{260}/A_{230} \geq 1.8$ and concentration > 50 ng/μl;
17 Thermo Fisher Scientific, Waltham, MA, USA). RNA integrity was checked by agarose
18 gel electrophoresis (1% TAE).

19 Six biological replicates of inoculated and three of mock-inoculated treatment were sent
20 to Macrogen Co. (Seoul, South Korea) for sequencing. Sequenced samples showed a
21 RNA integrity number (RIN) ≥ 7 measured by an Agilent 2100 Bioanalyzer. The strand-
22 specific RNA-Seq libraries were constructed using the Illumina TruSeq Stranded
23 mRNA protocol with polyadenylated mRNAs and lncRNAs enrichment and an insert

1 size of 300 bp (150x2 paired-end reads). Sequencing was performed on the Illumina
2 NovaSeq 6000 Sequencing System (Illumina Inc., USA).

3 2.3. Genome mapping and reference-based transcriptome assembly

4 All sequenced libraries were assessed for quality control using FastQC v.0.11.9
5 (Andrews 2012) and trimmed for Illumina adaptor sequences and low-quality base-calls
6 using Trimmomatic v.0.38 (Bolger *et al.* 2014). The trimmed reads with high quality
7 were then aligned to the *Pinus taeda* reference genome sequence (Pita_v2.01; Treegenes
8 database, Wegrzyn *et al.* 2008) using HISAT2 v.2.0.0 (Kim *et al.* 2015) with parameters
9 “--known-splicesite-infile”, “--dta” and “--rna-strandness RF”. In order to ensure the
10 presence of *F. circinatum* biomass in the samples, the reads were also mapped to its
11 publically available genome sequence (accession number JAGGEA000000000). The
12 SAM files from the pine mapping were processed with the SAMtools utility (Li *et al.*
13 2009) for converting to binary alignment map (BAM) format, sorting by coordinates
14 and removing duplicates. The transcripts for each sample were reconstructed separately
15 by StringTie v.2.1.4 (Pertea *et al.* 2015) using the “-G option” with the annotation file
16 of *P. taeda* (Pita.2_01.entap_annotations.tsv; Treegenes database, Wegrzyn *et al.* 2008).
17 This file was previously fixed with Gffread utility v.0.12.1 (Pertea and Pertea 2020) for
18 the correct understanding by StringTie program. After the transcriptome assembly, the
19 nine resulting GTF files were merged to generate a non-redundant set of transcripts with
20 unique identifiers using the StringTie “-merge” parameter, where only transcripts with
21 expression levels > 0.1 fragment per kilobase of exon per million mapped reads
22 (FPKM) were included. Finally, this newly experiment-level transcriptome was further
23 compared with the *P. taeda* reference annotation GTF file (Pita_v2.01; Treegenes
24 database, Wegrzyn *et al.* 2008) using the software Gffcompare v.0.12.1 (Pertea and

1 Pertea 2020), classifying transcripts in different class codes according to their
2 nature/origin.

3 2.4. LncRNAs identification

4 Based on all the assembled transcripts, the known transcripts marked with the class
5 code “=” were excluded before conducting the potential long non-coding RNAs
6 identification. The remaining transcripts were subjected to the coding potential predictor
7 FEELnc v.0.2 tool (Wucher *et al.* 2017) as well as several filters to ensure reliability of
8 lncRNAs. Firstly, the FEELnc filter module was used to remove short transcripts (< 200
9 nt) and retain monoexonic transcripts with antisense localization. After that, the
10 sequences of the resulting transcripts were extracted with Gffread v.0.12.1 (Pertea and
11 Pertea 2020) and the fasta file output was piped to the Eukaryotic Non-Model
12 Transcriptome Annotation Pipeline (EnTAP) v.0.9.2 (Hart *et al.* 2020) for transcript
13 annotation. Briefly, GeneMarkS-T v.5.1 (Tang *et al.* 2015) was used for open reading
14 frame (ORF) prediction and the sequence aligner DIAMOND v.1.9.2 (Buchfink *et al.*
15 2015) conducted the similarity search with default settings (E-value < 10^{-5}) using the
16 NCBI non-redundant protein database (release-201). After that, the assignment of
17 protein domains (Pfam), Gene Ontology (GO) terms and KEGG pathways was
18 performed using EggNOG v.1.0.3 (Huerta-Cepas *et al.* 2016). Finally, EnTAP filtered
19 contaminants to retain only high-quality transcripts. Subsequently, the FEELnc codpot
20 module was used with the shuffling mode to calculate a coding potential score (CPS)
21 for the un-annotated transcripts using a random forest algorithm trained with multi k-
22 mer frequencies and relaxed ORFs. The specificity threshold was set at 0.95 in order to
23 increase the robustness of the final set of novel lncRNAs. The remaining transcripts
24 were designated as lncRNAs and further classified according to the ‘Gffcompare’

1 output as long intergenic non-coding RNAs (lincRNAs) categorized with class code ‘u’,
2 long non-coding natural antisense transcripts (lncNAT) from the class code ‘x’, and
3 intronic transcripts that were those with class code ‘i’ (Budak *et al.* 2020).

4 In order to investigate the conservation of the pine lncRNAs, two recently released and
5 updated databases of known plant lncRNAs were used (Rai *et al.* 2019). All the
6 transcripts designated as lncRNA were aligned against CANTATA database
7 (Szcześniak *et al.* 2019) and GreeNc database (Gallart *et al.* 2016) using the blastn
8 algorithm (E-value $<10^{-5}$) of the BLAST v.2.9.0 software suite (Kozomara *et al.* 2019;
9 Kalvari *et al.* 2021). Moreover, the transcripts were also aligned to the Rfam (version
10 14.1) and miRBase (version 21) non-coding RNA databases with designated threshold
11 value (E-value $<10^{-5}$) using the blastn algorithm in order to detect housekeeping non-
12 coding RNAs including transfer RNA (tRNAs), ribosomal RNA (rRNAs) and
13 snoRNAs, and miRNA precursors.

14 2.5. Differential expression analysis

15 StringTie together with the “-e” parameter was employed to estimate expression for all
16 transcripts of the experiment-level transcriptome (Pertea *et al.* 2015). The output file
17 was reformatted using the “prepDE.py” script for further expression analysis (CCB
18 2019). DESeq2 v.1.24.1 (Love *et al.* 2014) was used to identify differentially expressed
19 (DE) lncRNA transcripts based on the matrix of the estimated counts. Differentially
20 expressed genes (DEG) were identified equally. The pairwise comparison of inoculated
21 and control plants were evaluated using Wald tests. To visualize the similarity of the
22 replicates and identify any sample outliers, the principal component analyses (PCA)
23 was constructed using the rlog-transformed expression values. Transcripts were
24 considered as differentially expressed if the adjusted p-values (padj) for multiple testing,

1 using Benjamini–Hochberg to estimate the false discovery rate (FDR) (Benjamini and
2 Hochberg 1995), was less than 0.05 and the $|\log_2(\text{Fold Change})| \geq 1$.

3 2.6. Potential target gene prediction and functional enrichment

4 Based on the genome location of the lncRNAs relative to the neighbouring genes, the
5 nearest protein-coding genes transcribed within a 10 kb window upstream or 100 kb
6 downstream were considered as potential *cis*-regulated target genes. These genes were
7 identified using the FEELnc classifier module (Wucher *et al.* 2017) and annotated using
8 the EnTAP pipeline (Hart *et al.* 2020) as described above but implemented with the
9 RefSeq complete protein database (release-201) and the UniProtKB/Swissprot database
10 (release-2020_05).

11 Functional enrichment analysis of the target genes associated with the DE lncRNAs was
12 conducted. DE lncRNA transcripts were divided into up- and down-regulated subsets
13 for efficient functional analysis (Hong *et al.* 2014). Using all genes as background, GO
14 and KEGG enrichment analysis were conducted by GOSep v.1.38.0 based on the
15 Wallenius non-central hyper-geometric distribution that allows the adjustment for
16 transcript length bias (Young *et al.* 2010). The GO terms and KEGG pathways with
17 corrected p-values lower than 0.05 were considered to be enriched in the group.
18 Redundant gene ontology categories were parsed using Revigo (Supek *et al.* 2011).

19 2.7. Co-expression analysis and identification of hub genes

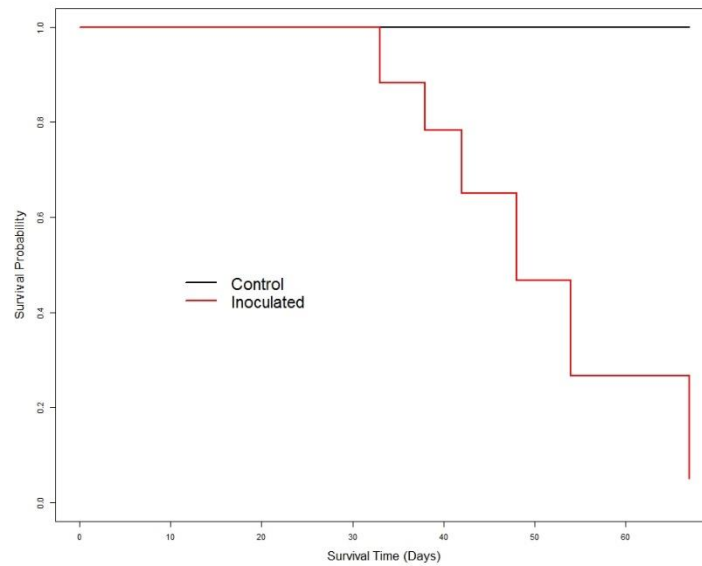
20 In order to predict the co-expression modules and determine the GO terms that
21 differentiate the transcriptome induced by *F. circinatum*, a weighted gene co-expression
22 network analysis approach implemented in the R-based Co-Expression Modules
23 identification Tool (CEMiTool) package v.1.8.3 (Russo *et al.* 2018) was conducted in R

1 software. Network analysis was carried out on the expression data for three gene sets:
2 DE lncRNAs, DEGs and targeted genes predicted by FEELnc. A variance stabilizing
3 transformation (vst) was used and transcripts were filtered to reduce correlation between
4 variance and gene expression. The Spearman's method was used for calculating the
5 correlation coefficients and a soft thresholding power (β) of 6 was selected. The co-
6 expressed modules were subjected to over-representation analysis (ORA) based on the
7 hypergeometric test (Yu *et al.* 2012) using the GO terms to determine the most
8 significant module functions ($q\text{-value} \leq 0.05$) (Russo *et al.* 2018). Moreover, genes with
9 the highest connectivity, known as hub genes and considered functionally-important
10 genes (Tahmasebi *et al.* 2019) were identified in each module.

11 **3. Results**

12 3.1. Disease monitoring

13 The survival analysis revealed clear significant differences between the inoculation and
14 control conditions ($\chi^2 = 116$, $p < 0.001$). At 10 dpi all seedlings inoculated with *F.*
15 *circinatum* showed symptoms of PPC (resin and/or necrosis at the stem and wilting) and
16 started to die at 33 dpi (**Figure 1**). By the end of the experiment, 92.2% of the
17 inoculated seedlings had died. No mortality was recorded for control seedlings.



1

2 **Figure 1.** Survival probability plot for *P. radiata* seedlings inoculated with *F.*
3 *circinatum* and mock-inoculated, determined using the Kaplan-Meier estimate of the
4 survival function.

5 3.2. Deep sequencing and transcripts assembly

6 High-throughput strand-specific RNA-Seq of nine libraries constructed from stem tissue
7 of *P. radiata* inoculated with *F. circinatum* and mock-inoculated were analysed. Raw
8 data of the experiment have been deposited at the NCBI under the SRA numbers
9 SRR15100123-31 (BioProject PRJNA742852). Almost 590 million 150-base pair-end
10 reads on polyadenylated selected (polyA) RNAs were generated by the Illumina
11 platform. RNA-Seq reached average depths of *ca.* 65.5 million reads (55 to 84 million
12 reads) (**Table S1**). After adapter and low-quality nucleotides trimming, an average of
13 78% of paired reads and 11% of mates from broken pairs were retained. Approximately
14 74.21% and 70.33% of reads from inoculated and mock-inoculated libraries
15 successfully mapped to the *P. taeda* reference genome, respectively (**Table S1**).

1 Considering the infected samples, the average of 2.63% reads mapped to the *F.*
 2 *circinatum* genome confirmed the presence of the pathogen.

3 Nine high-depth transcriptomes were generated. Six of them were reconstructed from *P.*
 4 *radiata* inoculated with *F. circinatum*, and the other three were generated from the
 5 mock-inoculated seedlings. After merging all of them, the unique transcriptome
 6 assembled were composed of 87,427 loci and 127,677 transcripts, with 43.1% GC
 7 content. A total of 51,212 (40.11%) transcripts were shared with the reference
 8 annotation file (Pita_v2.01.gtf) and discarded for lncRNA detection analysis since these
 9 transcripts were known as protein-coding RNAs. The remaining 76,465 transcripts were
 10 further categorized into different class codes according to its relationship with its closest
 11 reference transcript (**Table 1**).

12 **Table 1.** Number of unknown transcripts of *P. radiata* associated to a class code
 13 according to GffCompare software classification.

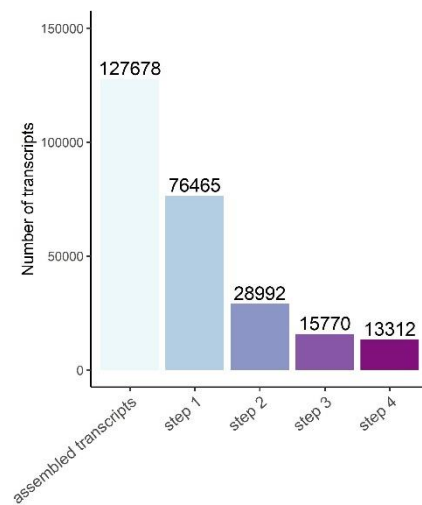
Class code	After assembly		LncRNAs predicted		Description ¹
	Transcript no.	%	Transcript no.	%	
x	902	0.71	446	3.35	Overlapping an exon of an annotated gene at the opposite strand
i	1,178	0.92	383	2.88	Fully contained in a known intron
y	500	0.39	189	1.42	Contains a reference gene within its intron
p	516	0.4	0	0	Adjacent to the 5' end of an annotated gene at the same strand
u	45,705	35.8	12,280	92.32	Intergenic region

14 ¹Brief explanation of the class codes.

15 3.3. Genome-wide identification and characterization of pine lncRNAs

16 The 76,465 total unknown transcripts were subjected to several sequential filter steps to
 17 obtain the lncRNA transcripts (**Figure 2**). A total of 13,312 lncRNAs (length \geq 200 nt,

1 ORF coverage < 50%, and potential coding score < 0.5) and 47,473 potential new
2 isoforms were obtained at the end of the pipeline. Using the FEELclassifier module, the
3 class distributions of the pine lncRNAs was performed according to their location
4 relative to the nearest protein-coding gene based on the reconstructed transcriptome.
5 The majority of the lncRNAs were lincRNAs with 12,291 (92.3%) transcripts, followed
6 by lncNAT with 445 (3.3%) transcripts and 383 (2.9%) intronic transcripts. In addition,
7 25 lncRNAs were also identified as known miRNA precursors belonging to 10 miRNA
8 families being the most represented MIR160, MIR159 and MIR1314. The Rfam and
9 miRBase analyses also allowed the identification of 174 transcripts that were found to
10 be distributed among 32 conserved RNA families including rRNA, tRNA, histones and
11 several snoRNAs (**Table S2-S3**).

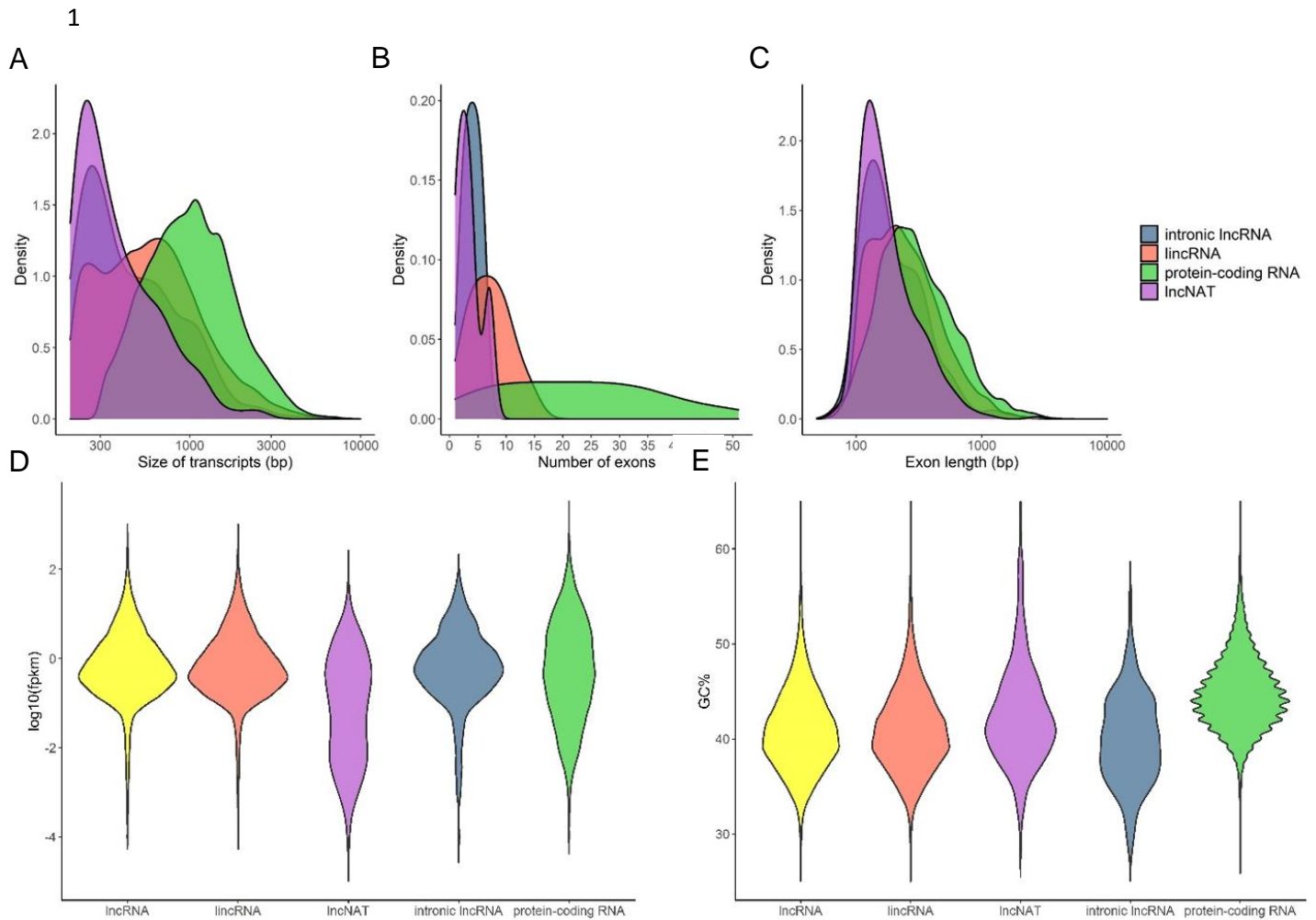


12

13 **Figure 2.** Statistics of candidate lncRNA transcripts. Step 1: known protein-coding
14 transcripts were filtered out. Step 2: transcripts with length ≥ 200 bp and with at least
15 two exons (including monoexonic transcripts with antisense localization) were selected.
16 Step 3: transcripts annotated with EnTAP program were filtered out. Step 4: with a
17 coding potential score lower than < 0.5 were retained.

1 The average length of protein-coding transcripts (1,200 bp) was higher than that of
2 lincRNAs (750 bp), lincNATs (452 bp) and intronic lincRNAs (565 bp). However, while
3 most of lincNATs and intronic lincRNAs showed short lengths (300 bp), lincRNAs and
4 protein-coding transcripts exhibited a similar trend of length distribution (**Figure 3A**).
5 Overall, the size distribution of the lincRNAs ranged from 200 to 7,393 bp, with the
6 majority of these transcripts ranging from 200 to 400 bp. Differences in the analysis of
7 the exon number were also found. While the lincRNAs showed an average exon number
8 of 2.5, the protein-coding transcripts had 4.1 exons (**Figure 3B**). This analysis also
9 revealed that two-exon transcripts were the most represented in this study. The highest
10 ratio of two-exon transcripts was found in lincNATs (77.3%) and intronic lincRNAs
11 (75.7%), followed by lincRNAs (66.9%). In the group of protein-coding transcripts, the
12 ratio of two-exon transcripts was not so high (32%). Regarding the exon length,
13 similarly to the transcript length, the exons belonging to the lincNAT and intronic
14 lincRNA transcripts showed shorter lengths (100-300 bp) than those belonging to
15 protein-coding transcripts (**Figure 3C**). Once again, the distribution of the exon lengths
16 from the lincRNA transcripts was similar to that of protein-coding transcripts.

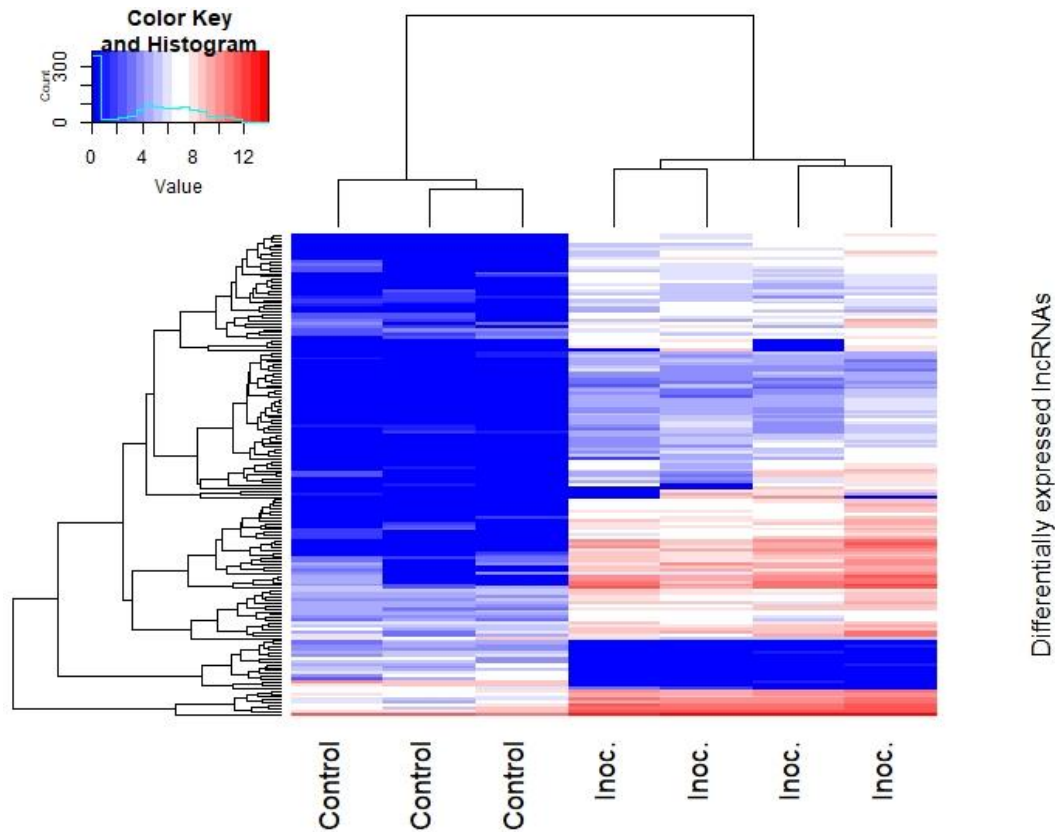
17 The average expression levels of lincRNAs in terms of FPKM was lower (3.3) than
18 those of protein-coding transcripts (5.6) (**Figure 3D**). In addition, the GC content in
19 lincRNAs (41%) was slightly lower than that in protein-coding transcripts (44.8%),
20 showing the intronic lincRNA transcripts the lowest percentage (**Figure 3E**).



1 *Populus trichocarpa*, *Prunus persica* and *Ananas comosus*. Likewise, known lncRNAs
2 of all plant species present in the GreeNc database, except those species already
3 examined with the CANTATA database, were confronted with the lncRNAs of *P.*
4 *radiata*. A number of 1,131 (8.6%) lncRNAs were conserved across the ten species of
5 CANTATA (**Table S4**). In addition, a total of 1,421 (10.8%) lncRNA transcripts,
6 corresponding to known lncRNA genes from the GreeNc database (**Table S5**), were
7 obtained. Therefore, 2,552 (19.3%) lncRNAs showed homology with known lncRNAs
8 from other plant species. The highest homology ratio (number of hits of pine lncRNAs
9 with those of each plant species to the total number of lncRNAs of each plant species)
10 was observed with the woody plant *P. trichocarpa* (5.03%) (**Figure S1**).

11 3.4. Differentially expressed analysis in response to *F. circinatum* infection 12 and prediction of candidate target genes

13 The expression changes of lncRNAs between the *P. radiata* seedlings inoculated with
14 *F. circinatum* and controls were analysed. The PCA allowed to identify two sample
15 outliers among the pathogen-inoculated condition that were discarded for the
16 differential expression analysis (**Figure S2**). A total of 164 lncRNA transcripts were
17 identified as differentially expressed ($p\text{-value} < 0.05$, $\log_2(|\text{Fold-change}|) \geq 1$) under the
18 pathogen infection, 146 of which were up-regulated and 18 down-regulated (**Table S6-**
19 **S7**). Among the DE lncRNAs, 157 transcripts were lincRNA and the remainder were
20 two intronic lncRNAs, one lncNATs, and four lncRNAs containing a coding-protein in
21 its intron. DE lncRNAs were clustered in a heat map in order to visualize the expression
22 pattern of both conditions of the analysis (**Figure 4**). On the other hand, 2,369 protein-
23 coding RNA were up-regulated and 189 down-regulated by the pathogen infection
24 (**Table S8-S9**).



1

2 **Figure 4.** The hierarchical clustering plot shows the scaled expression levels of the
3 differentially expressed lncRNAs of *P. radiata* in response to *F. circinatum*. Different
4 columns represent different libraries, and different rows represent the differentially
5 expressed lncRNAs. Red: relatively high expression; Blue: relatively low expression.

6 3.5. Analysis of lncRNAs *cis*-interacting genes

7 To predict the role of *cis*-acting lncRNAs of *P. radiata* in response to *F. circinatum*, the
8 protein-coding transcripts located within a 10 kb window upstream and 100 kb
9 downstream were investigated. A total of 4,268 lncRNA–mRNA interaction pairs were
10 recorded by the FEELnc classifier module (**Table S10**). However, one lncRNA could
11 have more than one target gene, and a target gene could be the target of one or more
12 lncRNAs. In fact, a number of 2,760 candidate *cis* target genes were observed for 3,750
13 lncRNAs, of which 3,342 had a single candidate target gene and 408 lncRNAs had

1 multiple interactions. The maximum number of target genes for a single lncRNA was
2 five, which was reached by seven lncRNAs (**Table S11**). Moreover, the 73% of the
3 2,760 candidate target genes were targeted by one lncRNA, while one candidate target
4 gene could be targeted by up to 30 different lncRNAs.

5 In total, 39 candidate target genes were predicted for the 37 DE lncRNAs (**Table 2**).
6 The function prediction of these DE lncRNAs was based on the functional annotation of
7 their nearby target genes. Among these targeted genes, there were genes encoding for
8 receptor-like protein kinases (RLKs), enzymes associated to the cell-wall reinforcement
9 and lignification (pectin methylesterases inhibitor, uclacyanin and 4-coumarate-CoA
10 ligase), and enzymes involved in the attenuation of oxidative stress (glutathione S-
11 transferase). One RLK that was predicted to be targeted by the up-regulated
12 lncRNAPiRa.29753.1 was, in turn, induced by the pathogen infection. Two pectin
13 methylesterases (PME) were predicted to be regulated by lncRNAPiRa.23041.2 and
14 lncRNAPiRa.22160.1 transcribed in the same orientation in a downstream location. One
15 of the targeted PME was DE by the pathogen infection, whereas the other PME did not.
16 Moreover, the coding region for 4-coumarate-CoA ligase 3 (4CL3) targeted by
17 lncRNAPiRa.33098.2 was also present among the DEGs of the coding RNAs analysis.
18 One gene harbouring the DNA-binding motif MYB, a transcription factor with a role in
19 plant stress tolerance, was potentially regulated by a lncNAT (lncRNAPiRa.31525.1).
20 The lncRNAPiRa.85000.6 lncRNA, which was predicted to target an ethylene receptor
21 2 (*ETR2*) gene involved in the ethylene signal transduction pathway, was transcribed in
22 the same strand and orientation than its RNA partner from an upstream location. In
23 addition, two genes encoding for photoassimilate-responsive protein 1 (PAR1) were
24 predicted to be targeted by lncRNAPiRa.61651.3 and lncRNAPiRa.33277.3, the latter
25 being DE between conditions.

1 The pine lncRNA lncRNAPiRa.79902.12 was predicted to target two genes encoding
 2 for the pyruvate decarboxylase 1 (PDC1) enzyme, which both were up-regulated by the
 3 pathogen infection. Furthermore, one gene that participates in chromatin modifications
 4 (chromatin remodelling 24) and three genes that contain canonical RNA-binding
 5 domains (pentatricopeptide repeat-containing protein, ribosomal RNA
 6 methyltransferase FtsJ domain containing protein, CCCH-type Znf protein) were
 7 predicted to be targeted in an antisense manner by lncRNAs. None of the three genes
 8 belonged to the DEGs.

9 **Table 2.** Candidate target genes predicted to interact with DE lncRNA transcripts.

LncRNA	Log ₂ FC	Targeted gene	Log ₂ FC	Direction	Type	Distance	Subtype	Location	Description of targeted gene
lncRNAPiRa.44237.18	9.76	PITA_00496		antisense	intergenic	41417	convergent	downstream	Pentatricopeptide repeat-containing protein At4g13650
lncRNAPiRa.64325.1	3.15	PITA_01014		antisense	genic	0	containing	exonic	Transcript with domain: DUF4228
lncRNAPiRa.32343.2	11.3	PITA_13284		antisense	intergenic	51151	convergent	downstream	CYCD2
lncRNAPiRa.35491.1	9.18	PITA_33574		antisense	intergenic	3155	convergent	downstream	Leaf rust 10 disease-resistance locus receptor-like protein kinase-like 1.2 isoform X1
lncRNAPiRa.42942.2	8.54	PITA_15284		antisense	intergenic	92774	divergent	upstream	Ribosomal RNA methyltransferase FtsJ domain-containing protein
lncRNAPiRa.22160.1	9.5	PITA_12411	6.58	sense	intergenic	9711	same_strand	downstream	Pectin methylesterase 17
lncRNAPiRa.31525.1	9.63	PITA_31792		antisense	intergenic	35358	convergent	downstream	Transcript with domain: Myb_DNA-binding
lncRNAPiRa.79902.12		PITA_05666	10.1	sense	genic	0	containing	intronic	PDC1
	7.12	PITA_12210	11.9	sense	intergenic	87	same_strand	downstream	PDC1
lncRNAPiRa.70333.4	7.9	PITA_01539		sense	genic	0	nested	intronic	Uclacyanin 1
lncRNAPiRa.51697.3	3.35	PITA_34628		sense	genic	0	containing	intronic	Transcript with domain: Peptidase_S28, Peptidase_S9
lncRNAPiRa.61651.3	8.53	PITA_42898		antisense	intergenic	7280	convergent	downstream	PAR1
lncRNAPiRa.33277.3	3.35	PITA_08467	3.54	sense	intergenic	376	same_strand	upstream	PAR1
lncRNAPiRa.45077.2	8.14	PITA_26106		antisense	intergenic	87766	convergent	downstream	Purple acid phosphatase
lncRNAPiRa.23041.2	9.27	PITA_28262		sense	intergenic	9586	same_strand	downstream	Pectin methylesterase 17
lncRNAPiRa.85490.1	6.99	PITA_28228		antisense	intergenic	85760	divergent	upstream	unknown [Picea sitchensis]
lncRNAPiRa.47042.1	7.53	PITA_13092		sense	intergenic	31121	same_strand	upstream	Transcript with domain: PP2C
lncRNAPiRa.19024.1	5.58	PITA_42377	5.17	sense	intergenic	542	same_strand	downstream	Non-symbiotic hemoglobin 1 (HB)
lncRNAPiRa.25700.7		PITA_23327		sense	genic	0	containing	intronic	Peptidase S9
	3.79	PITA_25465		sense	intergenic	541	same_strand	downstream	Prolyl endopeptidase
lncRNAPiRa.25968.1	2.91	PITA_42840	4.85	sense	intergenic	33267	same_strand	downstream	Transcript with domain: USP
lncRNAPiRa.29628.1	6.8	PITA_10474		sense	intergenic	812	same_strand	downstream	Transcript with domain: Glycolytic-Fructose-bisphosphate aldolase class-I
lncRNAPiRa.80857.1	6.78	PITA_28959		antisense	genic	0	nested	intronic	ALN

lncRNAPiRa.29753.1	7.2	PITA_38537	6.4	sense	intergenic	69405	same_strand	downstream	leaf rust 10 disease-resistance locus receptor-like protein kinase-like protein 2.4
lncRNAPiRa.33098.2	6.8	PITA_43179	5.01	sense	intergenic	6072	same_strand	downstream	4-coumarate-CoA ligase, partial (4CL3)
lncRNAPiRa.80336.1	4.89	PITA_17252		antisense	intergenic	47603	convergent	downstream	Protein chromatin remodeling 24
lncRNAPiRa.61651.4	5.82	PITA_42898		antisense	intergenic	7280	convergent	downstream	unknown [Picea sitchensis]
lncRNAPiRa.64704.5	6.91	PITA_22879		sense	intergenic	6023	same_strand	downstream	Lambda class glutathione S-transferase (GSTL1)
lncRNAPiRa.75647.1	5.93	PITA_04032		antisense	intergenic	8949	divergent	upstream	Transcript with domain: RRM_1
lncRNAPiRa.85000.6	9.91	PITA_16990		sense	intergenic	5468	same_strand	upstream	Ethylene receptor 2 (ETR2)
lncRNAPiRa.33190.1	7.85	PITA_44567		sense	intergenic	66345	same_strand	downstream	Transcript with domain: EamA
lncRNAPiRa.31184.1	2.25	PITA_16807		antisense	intergenic	55755	divergent	upstream	Transcript with domain: LEA_3
lncRNAPiRa.78332.11	2.65	PITA_41139	4.04	sense	genic	0	overlapping	intronic	CBS domain-containing protein cbscb3
lncRNAPiRa.42813.1	9.29	PITA_02986		sense	intergenic	190	same_strand	downstream	Hypothetical protein 0_9919_01, partial [Pinus taeda]
lncRNAPiRa.78487.3	9.39	PITA_28133		antisense	intergenic	33344	convergent	downstream	Transcript with domain: zf-CCCH
lncRNAPiRa.84511.1	4.53	PITA_13110	6.3	sense	intergenic	82	same_strand	downstream	Transcript with domain: Cellulase
lncRNAPiRa.62823.1	-9.14	PITA_01229		sense	intergenic	76300	same_strand	downstream	UBA52
lncRNAPiRa.83146.2	-7.43	PITA_05626		sense	intergenic	69363	same_strand	downstream	Pyridoxal kinase-like protein isoform X1
lncRNAPiRa.38350.3	-6.97	PITA_18454		sense	intergenic	494	same_strand	downstream	CC-NBS-LRR resistance-like protein

1 The enrichment analysis of GO terms and KEGG pathways of the nearby protein-

2 coding RNAs revealed potential functions in which DE lncRNAs could be involved

3 (**Figure 5**). The three target genes regulating the down-regulated lncRNAs were not

4 associated to any GO term neither KEGG pathway, thus the analysis showed results

5 only for the up-regulated lncRNAs (**Table S12**). Biological and metabolic processes

6 were the most representative GO terms for the biological process category, followed by

7 macromolecule metabolic process and response to stimulus and stress in this dataset.

8 Several GO terms associated with low-oxygen conditions including response to hypoxia

9 and response to decreased oxygen levels were enriched. In addition, catabolism and

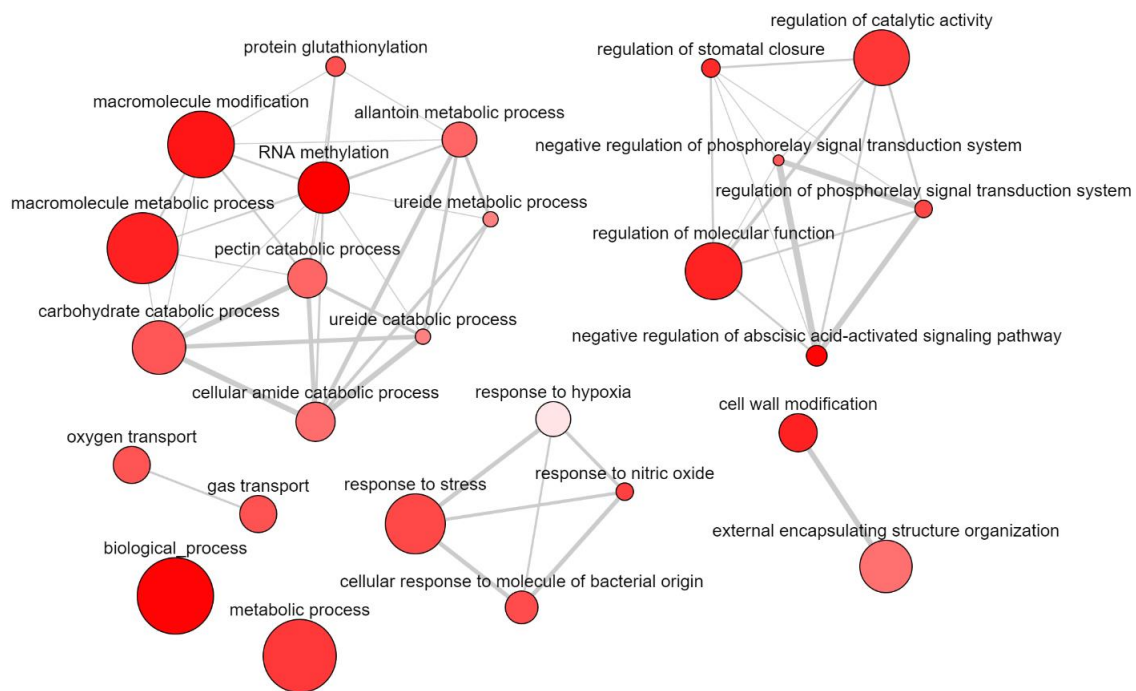
10 metabolism of allantoin were also enriched. Genes involved in cell periphery and cell

11 wall were represented for cellular components. For molecular functions, the pine

12 lncRNAs were enriched for GO terms such as catalytic activity, binding and hydrolase

13 activity. The KEGG pathways enriched in the target genes of the up-regulated lncRNAs

- 1 were ‘glycolysis/gluconeogenesis’ and ‘microbial metabolism in diverse environments’
- 2 (Table S13).



3

4 **Figure 5.** Enriched GO terms visualization of the DE lncRNA targeted genes
5 constructed by REVIGO. Connections are based on the structure of the GO hierarchy.
6 The colour of the bubble reflects the p-value obtained in the functional enrichment
7 analysis, while its size indicates the frequency of the GO term in the underlying
8 UniProt-GO Annotation database. Highly similar GO terms are linked by edges in the
9 graph, where the line width indicates the degree of similarity.

10 3.6. Co-expression gene modules associated with *P. radiata* defence 11 response

12 A dendrogram, in which the samples were clustered according to their condition using
13 the CEMiTool package, was generated (**Figure 6A**). The modular expression analysis
14 revealed genes that may act together or are similarly regulated during the defence

1 responses to *F. circinatum* infection. The dissimilarity threshold of 0.8 was used as a
2 cut-off on hierarchical clustering, which identified two co-expression modules (**Figure**
3 **6B-7C**). The largest module contained 320 co-expressed transcripts (M1): 307 DEGs,
4 13 DE lncRNAs, and three targeted genes (PDC1, PME and RLK) (**Table S14**).
5 Transcripts in M1 were enriched mainly for biological processes related to the
6 pectinesterase activity and cell wall remodeling among others (**Figure 6D**) (**Table S15**).
7 Indeed, three DEGs encoding for pectin methylesterase 17 were identified as gene hubs
8 in this module (**Table 3**). The second module (M2) consisted of 30 DEGs and one DE
9 lncRNA (**Table S14**), however, no significant GO terms were identified. The top gene
10 hubs of both modules are shown in **Table 3**.

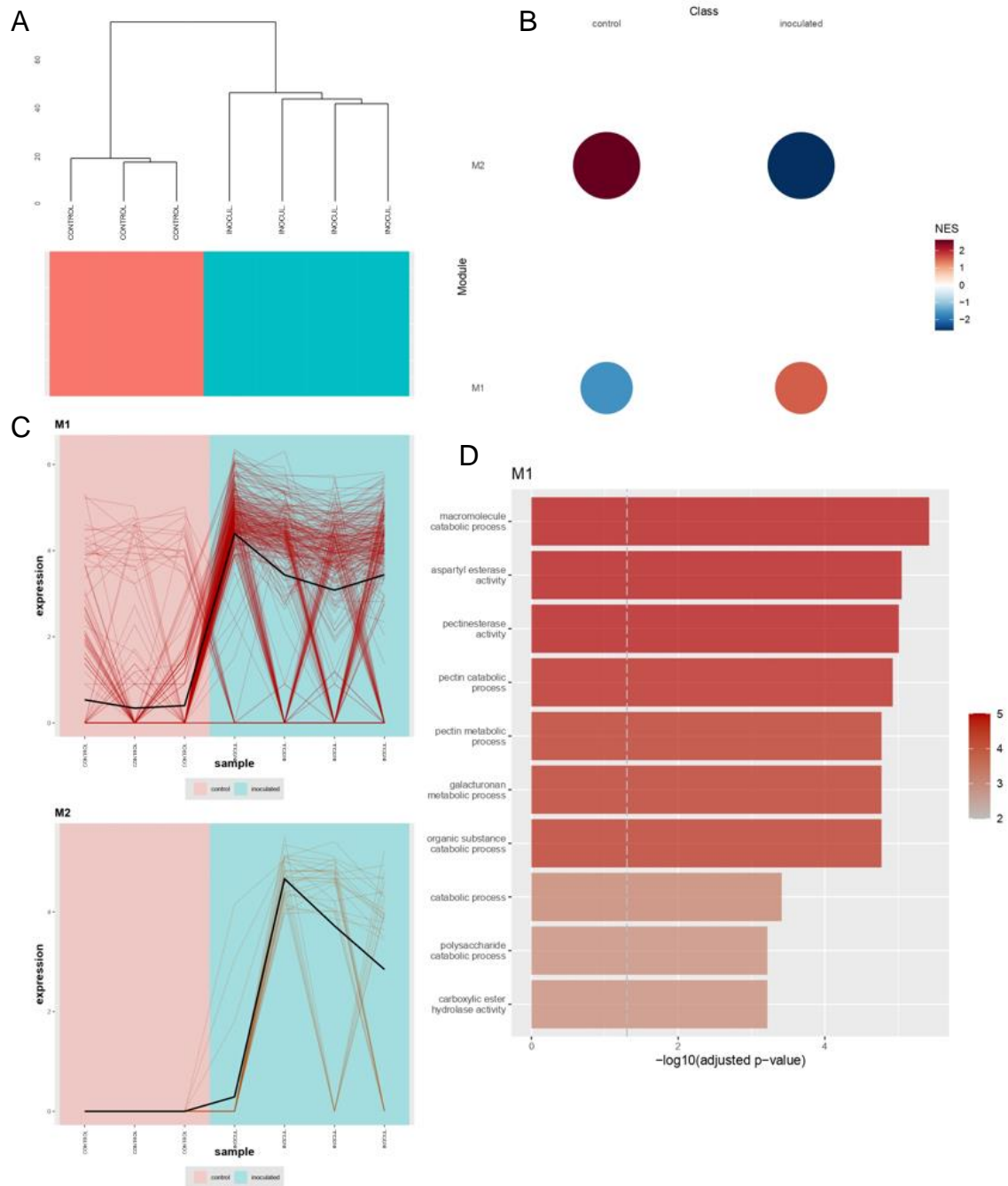


Figure 6. Two co-expression modules were identified among the DE lncRNAs, DEGs and targeted genes using CEMiTool package. (A) Dendrogram of samples clustered according to their condition. (B) Gene set enrichment analysis (GSEA)-based identification of two gene co-expression modules. Red coloring denotes a positive NES score, while blue coloring denotes a negative NES score. (C) Expression profiles for both expression modules (M1, M2). Each line represents a transcript and its change in

1 expression across conditions. (D) Barplot for top GO terms enriched in M1 module. *x*-
2 axis and colour transparency display - log₁₀ of the Benjamini-Hochberg (BH)-
3 adjusted p-value. Dashed vertical line indicates BH-adjusted p-value threshold of 0.05.

4 **Table 3.** Potential gene hubs of each co-expression gene module.

Transcript	Description
<i>Hub genes - M1</i>	
PITA.22172.1	Pectin methylesterase 17
PITA.22173.1	Pectin methylesterase 17
PITA_04671	Pectin methylesterase 17
PITA.84236.10	Alcohol dehydrogenase, partial (ADH1)
PITA_08271	Early nodulin-93-like
<i>Hub genes - M2</i>	
PITA.37728.4	2-methylene-furan-3-one reductase
PITA.32347.3	unknown
PITA.69828.1	hypothetical protein
PITA.7538.2	Glutathione S-transferase, partial (GST)
PITA.87100.2	Pheophytinase, chloroplastic-like

5

6 **4. Discussion**

7 Over the past decade, the complexity of eukaryote genome expression has become
8 apparent mainly due to the development of next-generation sequencing technologies.
9 Particularly, the sequencing of RNA (RNA-Seq) has revealed an important part of non-
10 coding transcriptome that should not be ignored. Indeed, a large number of studies have
11 recently reported lncRNAs to be essential in the regulation of a wide range of biological
12 and molecular processes by activating their nearby protein-coding genes using a *cis*-
13 mediated mechanism or distant genes in a *trans*-acting manner (Geisler and Coller
14 2013). Stress conditions lead to transcriptomic reprogramming where lncRNAs also
15 play a key role. In plants, numerous lncRNAs under biotic stress have been identified to
16 date, although further studies for non-model plants are still required. In the last years,

1 the transcriptomic responses of conifers to fungal infections have been increasingly
2 studied. In particular, several transcriptomic studies have demonstrated that the *F.*
3 *circinatum* infection causes substantial changes in the pine gene expression (Visser *et al.*
4 *al.* 2015, 2018, 2019; Carrasco *et al.* 2017; Hernandez-Escribano *et al.* 2020; Zamora-
5 Ballesteros *et al.* 2021). However, to our knowledge, no reports investigating the long
6 non-coding RNAs of conifer trees in response to fungal attacks have been published so
7 far. The results reported here, therefore, provide a first insight into the regulatory
8 mechanisms of lncRNAs involved in defence reactions against *F. circinatum* of a highly
9 susceptible species such as *P. radiata*.

10 The combination of the strand-specific RNA-Seq approach and high coverage
11 sequencing (up to 84 million reads per sample) allowed the identification of lncRNAs
12 that are commonly expressed at low levels and lncNATs that would otherwise have
13 been difficult to find (Rai *et al.* 2019). Overall, a total of 13,312 lncRNAs were
14 identified from the *P. radiata* transcriptome, of which 164 were *F. circinatum*-
15 responsive lncRNAs comprised mainly by intergenic lncRNAs. This is consistent with
16 previous analyses where the number of lncRNAs in response to a biotic stress was
17 comparable. In *Paulownia tomentosa*, two similar studies found 112 and 110 lncRNAs
18 to be involved in phytoplasma infection (Wang *et al.* 2017; Fan *et al.* 2018). Similarly,
19 among 94 and 302 lncRNAs were identified in susceptible and resistant *M. acuminata*
20 roots in response to *F. oxysporum* f. sp. *cubense*, with the highest value in the resistant
21 roots after 51 hours post-inoculation (Li *et al.* 2017). The number of *S. sclerotiorum*-
22 responsive lncRNAs was slightly higher in *B. napus* with 662 at 24 h decreasing until
23 308 at 48h (Joshi *et al.* 2016). In addition, intergenic lncRNAs were also the most
24 abundant responsive transcripts in all these studies. Therefore, the pattern appears to
25 follow the same trend in conifer trees.

1 In general, lncRNAs demonstrate low and tissue-specific expression patterns and lack
2 of conservation (Quan *et al.* 2015; Yu *et al.* 2019; Chen *et al.* 2020). Indeed, lncRNAs
3 of *P. radiata* showed lower expression than the protein-coding RNAs, and only 19.3%
4 of them were conserved among 46 non-conifer plant species. However, the low level of
5 transcriptome conservation in *P. radiata* to angiosperms has also been shown in xylem
6 tissues (15-32%; E-value $\leq 10^{-5}$), compared with the highly conserved xylem
7 transcriptome within conifers (78-82%; E-value $\leq 10^{-5}$) (Li *et al.* 2010). Thus, it may
8 not be a characteristic of conifer lncRNAs. The genomic features of the lncRNA
9 transcripts of *P. radiata* were consistent with those previously characterized in other
10 organisms (Cabili *et al.* 2011). As expected, the lncRNAs were shorter in terms of
11 overall length and contained lower number of exons. The length of the exons was also
12 shorter in lncNATs and intronic lncRNAs when comparing with protein-coding RNAs,
13 however, the distribution of the length of exons belonging to lincRNAs was closer to
14 that of the protein-coding transcripts. In this regard, some exceptions have been found
15 in other plants such as cotton (*Gossypium arboretum*) and chickpea (*Cicer arietinum*)
16 where the exon length of the lincRNAs were even longer than protein-coding RNAs
17 (Zaynab *et al.* 2018). The GC content of the assembled transcripts of *P. radiata* (43.1%)
18 was similar to that of the transcriptome of other *Pinus* species such as *P. tecunumanii*
19 (44%) (Visser *et al.* 2018). Separately, the GC content in pine lncRNAs (41%) was
20 lower than in protein-coding RNAs (44.8%), which had been reported before as a
21 common feature of lncRNAs due to different evolutionary pressures in ORFs (Shuai *et*
22 *al.* 2014).

23 The role of lncRNAs in the positive or negative regulation of gene expression is well
24 known (Quan *et al.* 2015). One of the conserved mechanism of action of the lncRNAs is
25 their function as decoys by sequestering RNA-binding proteins (RBP), miRNAs or

1 chromatin-modifying complexes (Wang and Chang 2011). Thus, the lncRNA ultimately
2 inhibits its particular function. Several DE lncRNAs of *P. radiata* inoculated by *F.*
3 *circinatum* seem to fit into this functional mechanism. Four antisense lncRNAs were
4 predicted to target genes encoding RBPs including pentatricopeptide repeat-containing
5 protein (PPR2), ribosomal RNA methyltransferase FtsJ domain containing protein,
6 CCCH-type zinc finger protein and RNA recognition motif (RRM) containing protein.
7 Moreover, another antisense DE lncRNA was predicted to target a chromatin-
8 remodelling gene. Therefore, the reprogramming exerted by the infection of *F.*
9 *circinatum* on pine transcription affects not only the protein-coding genes, but also the
10 non-coding part of the genome.

11 The induction of plant defences is a complex biological process that causes a dramatic
12 transcriptomic reprogramming throughout the genome (Kovalchuk *et al.* 2013).
13 Previous studies have shown that a vast number of genes are either up- or down-
14 regulated in response to *F. circinatum* infection (Carrasco *et al.* 2017; Visser *et al.*
15 2019; Hernandez-Escribano *et al.* 2020; Zamora-Ballesteros *et al.* 2021). Several
16 functional groups of genes have repeatedly been identified as induced upon the
17 pathogen infection. These groups include signal perception and transduction,
18 biosynthesis of defence hormone and secondary metabolites, and cell wall
19 reinforcement and lignification. Some of the GO terms enriched by the lncRNAs
20 identified in this study were related to these functional groups including biological
21 processes such as cell wall modification and signalling of the abscisic acid, ethylene and
22 cytokinin hormones. These results suggest for the first time that the lncRNAs may play
23 a key role in the process of pine defence to *F. circinatum* as previously reported in other
24 pathosystems (Zhu *et al.* 2014; Sanchita *et al.* 2020).

1 Plant signalling molecules such as protein kinases, reactive oxygen species (ROS) and
2 hormones are critical in mounting an appropriate defence response (Yu *et al.* 2017).
3 Genes with kinase activity have a role in signal transduction triggering the downstream
4 signalling. Two genes with predicted functions in receptor-like kinase were *cis*-
5 regulated by lncRNAs, being one of them DE by the pathogen infection. The other one
6 was potentially regulated by a lncNAT. Positive *cis*-regulatory feature of NATs by
7 mediating histone modifications at the locus has been previously reported (Yu *et al.*
8 2019). This behaviour has been also seen in LAIR, a rice lncNAT that up-regulates the
9 expression of its neighbour leucine-rich repeat receptor kinase (Wang *et al.* 2018).
10 Despite that a large number of genes (43) encoding glutathione S-transferases (GSTs)
11 were up-regulated under the pathogen infection, the GST predicted to be regulated by
12 the downstream lncRNAPiRa.64704.1 was not among the DEGs. Joshi *et al.* (2016)
13 also identified one lncRNA of *B. napus* located in the upstream of a gene encoding for a
14 GST in response to *S. sclerotiorum* infection. GST genes are highly induced under
15 biotic stress due to their role in the attenuation of oxidative stress and the participation
16 in hormone transport (Gullner *et al.* 2018). In addition, a transcript predicted to encode
17 a non-symbiotic hemoglobin 1, which is involved in ROS and NO scavenging (Bahmani
18 *et al.* 2019), was DE in the analysis and predicted to be targeted by
19 lncRNAPiRa.19024.1. These findings seem to indicate that lncRNAs could be also
20 involved in the cell detoxification after an oxidative burst provoked by a fungal
21 infection.

22 Phytohormones trigger an effective defence response against biotic stress (Checker *et al.*
23 *et al.* 2018). Several studies have pointed to lncRNAs as participants in the complex
24 network of hormone regulation. In *M. acuminata* infected by *F. oxysporum* f. sp.
25 *cubense*, lncRNAs were found to be predominantly associated with auxin and salicylic

1 acid signal transduction in susceptible cultivars, whereas all phytohormones were
2 potentially regulated by lncRNAs in resistant cultivars (Li *et al.* 2017). Genes related to
3 the salicylic acid-mediated defence process were co-expressed with lncRNAs in
4 kiwifruit plant challenged with the bacteria *P. syringae* (Wang *et al.* 2017). Likewise,
5 lncRNAs of resistant walnuts to *C. gloeosporioides* were predicted to *trans*-regulate
6 genes involved in defence pathways of the jasmonic acid and auxins (Feng *et al.* 2021).
7 A previous transcriptome analysis of *P. radiata* showed the induction of abscisic acid
8 signalling under the infection of *F. circinatum* (Carrasco *et al.* 2017). A type 2C protein
9 phosphatase (PP2C) family gene, which negatively regulates abscisic acid responses
10 (Cao *et al.* 2016; Jung *et al.* 2020), could be regulated by lncRNAPiRa.47042.1 located
11 upstream in the same strand despite not belonging to the DEGs. The implication of this
12 lncRNA in the abscisic acid signalling regulation would need further investigation.

13 The phytohormone ethylene represents one of the core components of the plant immune
14 system (Müller and Munné-Bosch 2015). When ethylene binds with its ETRs activates
15 the transcriptional cascade of ethylene-regulated genes (Sakai *et al.* 1998). Seedlings of
16 *P. tecunumanii*, *P. patula*, *P. pinea* and *P. radiata* inoculated with *F. circinatum* have
17 demonstrated to induce ethylene biosynthesis and signalling genes (Carrasco *et al.*
18 2017; Visser *et al.* 2019; Zamora-Ballesteros *et al.* 2021); however, only *ETR2* has been
19 found to be induced in the moderate resistant specie *P. pinaster* at 5 and 10 dpi
20 (Hernandez-Escribano *et al.* 2020). Under stress conditions, when the concentration of
21 ethylene is high, the transcription of *ETR2* contributes to the stabilization of ethylene
22 levels by attenuating its signalling output and restore the ability to respond to
23 subsequent ethylene signal (Zhao and Guo 2011). In the present study, *ETR2* has not
24 been DE in *P. radiata* but was presumably influenced by lncRNAPiRa.85000.6, which
25 has been DE by *F. circinatum*. Therefore, we can hypothesize that the ethylene response

1 seems to be fine-tuned in *P. pinaster*, which does not occur in *P. radiata*, possibly due
2 to the influence of this lncRNA located upstream of its transcription. It would be
3 worthwhile to further investigate the regulatory function of this lncRNA as it could be a
4 key factor in overcoming the PPC disease.

5 The potential function of lncRNAs in wood formation has been previously observed in
6 different plant species. In a study of cotton lncRNAs, these were enriched for lignin
7 catabolic processes and their role in lignin biosynthesis by regulating the expression of
8 LAC4 was suggested (Wang *et al.* 2015). In *Populus*, 16 genes targeted by lncRNAs
9 were involved in wood formation processes, including lignin biosynthesis (Chen *et al.*
10 2015), and 13 targeted genes were associated to cellulose and pectin synthesis (Tian *et*
11 *al.* 2016). In addition, the lncRNA NERDL regulates the Needed for rdr2-independent
12 DNA methylation (*NERD*) gene, which is also involved in the wood formation in
13 *Populus* (Shi *et al.* 2017). The enzyme that catalyse the hemicellulose xyloglucan was
14 predicted to be targeted by a lncRNA of *Paulownia tomentosa* and had a role in the
15 hyperplasia caused by a phytoplasma infection (Zhe Wang *et al.* 2017). Cell wall
16 reinforcement and lignification are the most common induced defences against
17 pathogens, for that, the cell wall suffers a remodelling process that has been
18 documented in the *P. radiata-F. circinatum* pathosystem (Carrasco *et al.* 2017; Zamora-
19 Ballesteros *et al.* 2021). The demethylesterification of pectin, controlled by PMEs, is
20 considered to affect the porosity of the cell wall and, thus, exposes the plant to an easier
21 degradation by pathogen enzymes (Raiola *et al.* 2011). However, PME activity has been
22 also associated with the activation of plant immunity and resistance against pathogens
23 (Del Corpo *et al.* 2020). In a recent study, in contrast to *P. radiata*, the resistant species
24 *P. pinea* infected by *F. circinatum* showed a high induction of pectin methylesterase
25 inhibitor (PMEI) genes and an inhibition of PMEs (Zamora-Ballesteros *et al.* 2021). In

1 the present study, two lncRNAs were predicted to target two PME, one of them was
2 up-regulated by the pathogen infection, which could suggest a positive regulation from
3 the lncRNA activity. In addition, the co-expression analysis of *F. circinatum* responsive
4 lncRNAs and mRNAs indicated a clear enrichment for PME activity. The
5 transcriptional regulation of these enzymes could be related to the susceptibility of *P.*
6 *radiata* and would be worth further investigation. Another gene containing a cellulase
7 domain was also up-regulated in the expression analysis of protein-coding RNAs and
8 predicted to be regulated by an induced lncRNA. Moreover, the analysis identified a
9 potential lncRNA *cis*-regulating positively a gene encoding for 4CL3, one of the key
10 enzymes of the phenylpropanoid pathway. In plants, this pathway leads to the
11 production of secondary metabolites and cell wall lignification, both associated to plant
12 defence. The transcriptional regulation of the *4CL* gene by lncRNAs has been also
13 reported in *P. tomentosa*, that together with the targeted gene encoding the caffeoyl-
14 CoA 3-O-methyltransferase (CCOMT) enzyme by another lncRNA, highlighted the
15 potential role of these molecules in lignin formation in wood with different properties
16 (Chen *et al.* 2015). These findings provide increasing evidence for the involvement of
17 lncRNAs in cell wall remodelling and lignification process.

18 Although the role of the hypoxia in the plant-pathogen interaction has not yet been
19 determined, hypoxia-responsive genes have been reported to be induced in some plants
20 during pathogen infections (Loreti and Perata 2020). Indeed, the analysis of DEGs
21 showed that a large number of genes encoding for PDC1 and alcohol dehydrogenase 1
22 (ADH1), which are required in the fermentative pathway under low-oxygen conditions,
23 were highly induced by *F. circinatum* infection ($>10 \log_2$ [fold change]; **Table S8**).
24 Among them, two PDC1 were potentially targeted by two pine lncRNAs. This together
25 with the functional analysis results of the lncRNAs where several enriched GO terms

1 were associated to hypoxia suggests a role of pine lncRNAs in an insufficient oxygen
2 situation.

3 In summary, the computational analysis allowed to identify 13,312 lncRNAs in *P.*
4 *radiata*. Compared to the protein-coding RNAs, the lncRNAs were shorter, with fewer
5 exons and showed lower expression levels. In total 164 lncRNAs were reported as
6 responsive to *F. circinatum* infection. GO enrichment of genes that either overlap with
7 or are neighbours of these pathogen-responsive lncRNAs suggested involvement of
8 important defence processes including signal transduction and cell wall reinforcement.
9 These results present a comprehensive map of lncRNAs in *P. radiata* under *F.*
10 *circinatum* infection and provide a starting point to understand their regulatory
11 mechanisms and functions in conifer defence. In turn, a thorough understanding of the
12 mechanism of gene regulation will contribute to the improvement of breeding programs
13 for resistant pine commercialization, one of the most promising approaches for PPC
14 management.

15 5. References

16 **Andrews S. 2012.** *FastQC a quality control tool for high throughput sequence data.*
17 <http://www.bioinformatics.babraham.ac.uk/projects/fastqc/>. 28 Feb. 2020.

18 **Bahmani R, Kim DG, Na JD, Hwang S. 2019.** Expression of the tobacco non-
19 symbiotic class 1 hemoglobin gene *hb1* reduces cadmium levels by modulating cd
20 transporter expression through decreasing nitric oxide and ROS level in *Arabidopsis*.
21 *Frontiers in Plant Science* **10**: 201.

22 **Benjamini Y, Hochberg Y. 1995.** Controlling the False Discovery Rate: A Practical
23 and Powerful Approach to Multiple. *Journal of the Royal Statistical Society. Series B*
24 *(Methodological)* **57**: 289–300.

- 1 **Bolger AM, Lohse M, Usadel B. 2014.** Trimmomatic: A flexible trimmer for Illumina
2 sequence data. *Bioinformatics* **30**: 2114–2120.
- 3 **Bonnet E, Van de Peer Y, Rouzé P. 2006.** The small RNA world of plants. *New*
4 *Phytologist* **171**: 451–468.
- 5 **Buchfink B, Xie C, Huson DH. 2015.** Fast and sensitive protein alignment using
6 DIAMOND. *Nature Methods* **12**: 59–60.
- 7 **Budak H, Kaya SB, Cagirici HB. 2020.** Long Non-coding RNA in Plants in the Era of
8 Reference Sequences. *Frontiers in Plant Science* **11**: 276.
- 9 **Cabili M, Trapnell C, Goff L, et al. 2011.** Integrative annotation of human large
10 intergenic noncoding RNAs reveals global properties and specific subclasses. *Genes*
11 *and Development* **25**: 1915–1927.
- 12 **Cao J, Jiang M, Li P, Chu Z. 2016.** Genome-wide identification and evolutionary
13 analyses of the *PP2C* gene family with their expression profiling in response to multiple
14 stresses in *Brachypodium distachyon*. *BMC Genomics* **17**: 175.
- 15 **Carrasco A, Wegrzyn JL, Durán R, et al. 2017.** Expression profiling in *Pinus radiata*
16 infected with *Fusarium circinatum*. *Tree Genetics and Genomes* **13**.
- 17 **CCB. 2019.** *StringTie*. <http://ccb.jhu.edu/software/stringtie/index.shtml?t=manual>. 7
18 Jul. 2021.
- 19 **Checker VG, Kushwaha HR, Kumari P, Yadav S. 2018.** Role of phytohormones in
20 plant defense: Signaling and cross talk In: Singh A, Singh I, eds. *Molecular Aspects of*
21 *Plant-Pathogen Interaction*. Singapore: Springer , 159–184.
- 22 **Chen J, Quan M, Zhang D. 2015.** Genome-wide identification of novel long non-
23 coding RNAs in *Populus tomentosa* tension wood, opposite wood and normal wood

- 1 xylem by RNA-seq. *Planta* **241**: 125–143.
- 2 **Chen L, Zhu QH, Kaufmann K. 2020.** Long non-coding RNAs in plants: emerging
3 modulators of gene activity in development and stress responses. *Planta* **252**: 92.
- 4 **Del Corpo D, Fullone MR, Miele R, et al. 2020.** AtPME17 is a functional *Arabidopsis*
5 *thaliana* pectin methylesterase regulated by its PRO region that triggers PME activity in
6 the resistance to *Botrytis cinerea*. *Molecular Plant Pathology* **21**: 1620–1633.
- 7 **Drenkhan R, Ganley B, Martín-García J, et al. 2020.** Global Geographic Distribution
8 and Host Range of *Fusarium circinatum*, the Causal Agent of Pine Pitch Canker.
9 *Forests* **11**.
- 10 **Fan G, Cao Y, Wang Z. 2018.** Regulation of long noncoding RNAs responsive to
11 phytoplasma infection in *Paulownia tomentosa*. *International Journal of Genomics*.
- 12 **Feng S, Fang H, Liu X, Dong Y, Wang Q, Yang KQ. 2021.** Genome-wide
13 identification and characterization of long non-coding RNAs conferring resistance to
14 *Colletotrichum gloeosporioides* in walnut (*Juglans regia*). *BMC Genomics* **22**: 15.
- 15 **Franco-Zorrilla JM, Valli A, Todesco M, et al. 2007.** Target mimicry provides a new
16 mechanism for regulation of microRNA activity. *Nature Genetics* **39**: 1033–1037.
- 17 **Gallart AP, Pulido AH, De Lagrán IAM, Sanseverino W, Cigliano RA. 2016.**
18 GREENC: A Wiki-based database of plant lncRNAs. *Nucleic Acids Research* **44**:
19 D1161–D1166.
- 20 **Geisler S, Coller J. 2013.** RNA in unexpected places: Long non-coding RNA functions
21 in diverse cellular contexts. *Nature Reviews Molecular Cell Biology* **14**: 699–712.
- 22 **Gil N, Ulitsky I. 2020.** Regulation of gene expression by *cis*-acting long non-coding
23 RNAs. *Nature Reviews Genetics* **21**: 102–117.

- 1 **Gordon TR, Swett CL, Wingfield MJ. 2015.** Management of *Fusarium* diseases
2 affecting conifers. *Crop Protection* **73**: 28–39.
- 3 **Gullner G, Komives T, Király L, Schröder P. 2018.** Glutathione S-transferase
4 enzymes in plant-pathogen interactions. *Frontiers in Plant Science* **9**: 1836.
- 5 **Hart AJ, Ginzburg S, Xu M (Sam), et al. 2020.** EnTAP: Bringing faster and smarter
6 functional annotation to non-model eukaryotic transcriptomes. *Molecular Ecology*
7 *Resources* **20**: 591–604.
- 8 **Heo JB, Sung S. 2011.** Vernalization-mediated epigenetic silencing by a long intronic
9 noncoding RNA. *Science* **331**: 76–79.
- 10 **Hernandez-Escribano L, Visser EA, Iturritxa E, Raposo R, Naidoo S. 2020.** The
11 transcriptome of *Pinus pinaster* under *Fusarium circinatum* challenge. *BMC Genomics*
12 **21**: 1–18.
- 13 **Hong G, Zhang W, Li H, Shen X, Guo Z. 2014.** Separate enrichment analysis of
14 pathways for up- and downregulated genes. *Journal of the Royal Society Interface* **11**:
15 20130950.
- 16 **Hou X, Cui J, Liu W, et al. 2020.** LncRNA39026 enhances tomato resistance to
17 *Phytophthora infestans* by decoying miR168a and inducing PR gene expression.
18 *Phytopathology* **110**: 873–880.
- 19 **Huerta-Cepas J, Szklarczyk D, Forslund K, et al. 2016.** EGGNOG 4.5: A
20 hierarchical orthology framework with improved functional annotations for eukaryotic,
21 prokaryotic and viral sequences. *Nucleic Acids Research* **44**: D286–D293.
- 22 **Joshi RK, Megha S, Basu U, Rahman MH, Kav NN V. 2016.** Genome Wide
23 Identification and Functional Prediction of Long Non-Coding RNAs Responsive to

- 1 *Sclerotinia sclerotiorum* Infection in *Brassica napus* (B Shan, Ed.). *PLOS ONE* **11**:
2 e0158784.
- 3 **Jung C, Nguyen NH, Cheong JJ. 2020.** Transcriptional regulation of protein
4 phosphatase 2c genes to modulate abscisic acid signaling. *International Journal of*
5 *Molecular Sciences* **21**: 1–18.
- 6 **Kalvari I, Nawrocki EP, Ontiveros-Palacios N, et al. 2021.** Rfam 14: Expanded
7 coverage of metagenomic, viral and microRNA families. *Nucleic Acids Research* **49**:
8 D192–D200.
- 9 **Kaplan EL, Meier P. 1958.** Nonparametric Estimation from Incomplete Observations.
10 *Journal of the American Statistical Association* **53**: 481.
- 11 **Kapranov P, Cheng J, Dike S, et al. 2007.** RNA maps reveal new RNA classes and a
12 possible function for pervasive transcription. *Science* **316**: 1484–1488.
- 13 **Kim D, Langmead B, Salzberg SL. 2015.** HISAT: A fast spliced aligner with low
14 memory requirements. *Nature Methods* **12**: 357–360.
- 15 **Kovalchuk A, Kerio S, Oghenekaro AO, Jaber E, Raffaello T, Asiegbu FO. 2013.**
16 Antimicrobial Defenses and Resistance in Forest Trees: Challenges and Perspectives in
17 a Genomic Era. *Article in Annual Review of Phytopathology* **51**: 221–44.
- 18 **Kozomara A, Birgaoanu M, Griffiths-Jones S. 2019.** MiRBase: From microRNA
19 sequences to function. *Nucleic Acids Research* **47**: D155–D162.
- 20 **Li H, Handsaker B, Wysoker A, et al. 2009.** The Sequence Alignment/Map format
21 and SAMtools. *Bioinformatics Applications Note* **25**: 2078–2079.
- 22 **Li W, Li C, Li S, Peng M. 2017.** Long noncoding RNAs that respond to *Fusarium*
23 *oxysporum* infection in “Cavendish” banana (*Musa acuminata*). *Scientific Reports* **7**: 1–

- 1 13.
- 2 **Li X, Wu HX, Southerton SG. 2010.** Comparative genomics reveals conservative
3 evolution of the xylem transcriptome in vascular plants. *BMC Evolutionary Biology* **10**:
4 1–14.
- 5 **Liu X, Hao L, Li D, Zhu L, Hu S. 2015.** Long Non-coding RNAs and Their Biological
6 Roles in Plants. *Genomics, Proteomics and Bioinformatics* **13**: 137–147.
- 7 **Loreti E, Perata P. 2020.** The Many Facets of Hypoxia in Plants. *Plants* **9**: 745.
- 8 **Love MI, Huber W, Anders S. 2014.** Moderated estimation of fold change and
9 dispersion for RNA-seq data with DESeq2. *Genome Biology* **15**: 550.
- 10 **Lozada-Chávez I, Stadler PF, Prohaska SJ. 2011.** “Hypothesis for the Modern RNA
11 World”: A pervasive Non-coding RNA-Based Genetic Regulation is a Prerequisite for
12 the Emergence of Multicellular Complexity. *Origins of Life and Evolution of*
13 *Biospheres* **41**: 587–607.
- 14 **Ma L, Bajic VB, Zhang Z. 2013.** On the classification of long non-coding RNAs. *RNA*
15 *Biology* **10**: 924–933.
- 16 **Martin-Garcia J, Paraschiv M, Asdrubal Flores-Pacheco J, Chira D, Javier Diez J,**
17 **Fernandez M. 2017.** Susceptibility of Several Northeastern Conifers to *Fusarium*
18 *circinatum* and Strategies for Biocontrol. *Forests* **8**: 318.
- 19 **Martín-García J, Zas R, Solla A, et al. 2019.** Environmentally-friendly methods for
20 controlling pine pitch canker. *Plant Pathology* **68**: 843–860.
- 21 **Müller M, Munné-Bosch S. 2015.** Ethylene Response Factors: A Key Regulatory Hub
22 in Hormone and Stress Signaling. *Plant Physiology* **169**: 32–41.

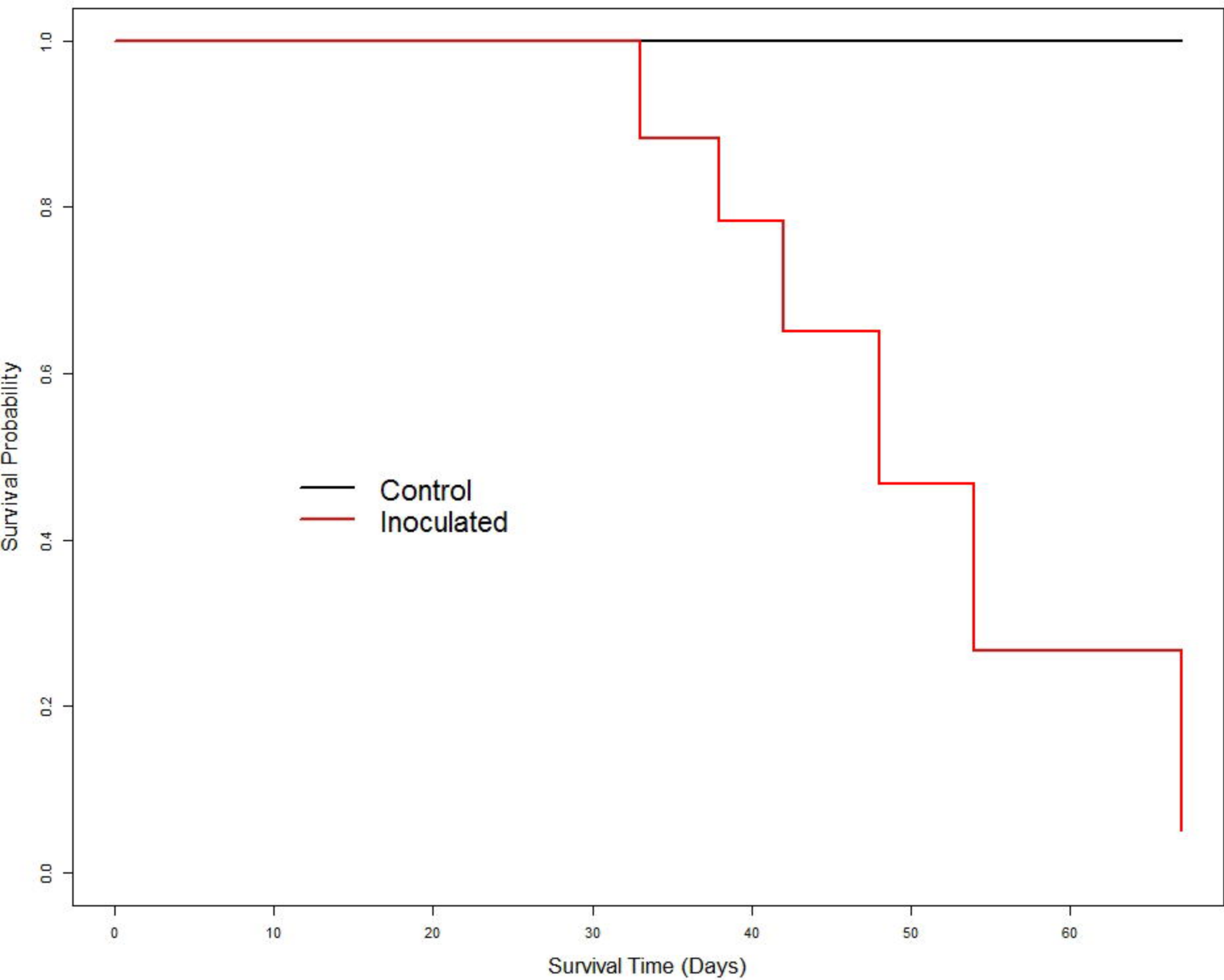
- 1 **Pertea M, Pertea G. 2020.** GFF Utilities: GffRead and GffCompare. *F1000Research* **9**:
2 304.
- 3 **Pertea M, Pertea GM, Antonescu CM, et al. 2015.** StringTie enables improved
4 reconstruction of a transcriptome from RNA-seq reads. *Nat Biotechnol* **33**: 290–295.
- 5 **Qin T, Zhao H, Cui P, Albeshar N, Xiong L. 2017.** A nucleus-localized long non-
6 coding RNA enhances drought and salt stress tolerance. *Plant Physiology* **175**: 1321–
7 1336.
- 8 **Quan M, Chen J, Zhang D. 2015.** Exploring the secrets of long noncoding RNAs.
9 *International Journal of Molecular Sciences* **16**: 5467–5496.
- 10 **R Core Team. 2019.** *R: The R Project for Statistical Computing*. [https://www.r-](https://www.r-project.org/)
11 [project.org/](https://www.r-project.org/). 16 Nov. 2020.
- 12 **Rai MI, Alam M, Lightfoot DA, Gurha P, Afzal AJ. 2019.** Classification and
13 experimental identification of plant long non-coding RNAs. *Genomics* **111**: 997–1005.
- 14 **Raiola A, Lionetti V, Elmaghraby I, et al. 2011.** Pectin methylesterase is induced in
15 *Arabidopsis* upon infection and is necessary for a successful colonization by
16 necrotrophic pathogens. *Molecular Plant-Microbe Interactions* **24**: 432–440.
- 17 **Russo PST, Ferreira GR, Cardozo LE, et al. 2018.** CEMiTool: A Bioconductor
18 package for performing comprehensive modular co-expression analyses. *BMC*
19 *Bioinformatics* **19**: 1–13.
- 20 **Sakai H, Hua J, Chen QG, et al. 1998.** *ETR2* is an *ETR1*-like gene involved in
21 ethylene signaling in *Arabidopsis*. *Proceedings of the National Academy of Sciences of*
22 *the United States of America* **95**: 5812–5817.
- 23 **Sanchita, Trivedi PK, Asif MH. 2020.** Updates on plant long non-coding RNAs

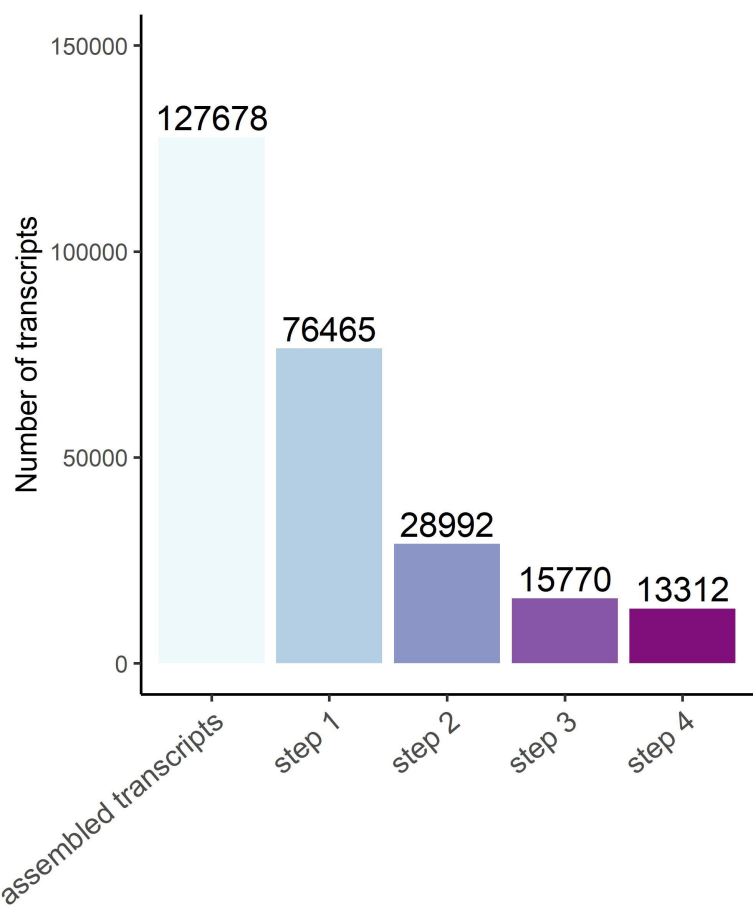
- 1 (lncRNAs): the regulatory components. *Plant Cell, Tissue and Organ Culture* **140**: 259–
2 269.
- 3 **Seo JS, Sun HX, Park BS, et al. 2017.** ELF18-INDUCED LONG-NONCODING
4 RNA associates with mediator to enhance expression of innate immune response genes
5 in *Arabidopsis*. *Plant Cell* **29**: 1024–1038.
- 6 **Shi W, Quan M, Du Q, Zhang D. 2017.** The Interactions between the Long Non-
7 coding RNA NERDL and Its Target Gene Affect Wood Formation in *Populus*
8 *tomentosa*. *Frontiers in Plant Science* **8**: 1035.
- 9 **Shuai P, Liang D, Tang S, et al. 2014.** Genome-wide identification and functional
10 prediction of novel and drought-responsive lincRNAs in *Populus trichocarpa*. *Journal*
11 *of Experimental Botany* **65**: 4975–4983.
- 12 **Supek F, Bošnjak M, Škunca N, Šmuc T. 2011.** REVIGO Summarizes and Visualizes
13 Long Lists of Gene Ontology Terms (C Gibas, Ed.). *PLoS ONE* **6**: e21800.
- 14 **Swiezewski S, Liu F, Magusin A, Dean C. 2009.** Cold-induced silencing by long
15 antisense transcripts of an *Arabidopsis* Polycomb target. *Nature* **462**: 799–803.
- 16 **Szcześniak MW, Bryzghalov O, Ciomborowska-Basheer J, Makalowska I. 2019.**
17 CANTATAdb 2.0: Expanding the Collection of Plant Long Noncoding RNAs In:
18 Chekanova JA, Wang HV, eds. *Methods in Molecular Biology*. New York, NY:
19 Humana Press Inc., 415–429.
- 20 **Tahmasebi A, Ashrafi-Dehkordi E, Shahriari AG, Mazloomi SM, Ebrahimie E.**
21 **2019.** Integrative meta-analysis of transcriptomic responses to abiotic stress in cotton.
22 *Progress in Biophysics and Molecular Biology* **146**: 112–122.
- 23 **Tang S, Lomsadze A, Borodovsky M. 2015.** Identification of protein coding regions in

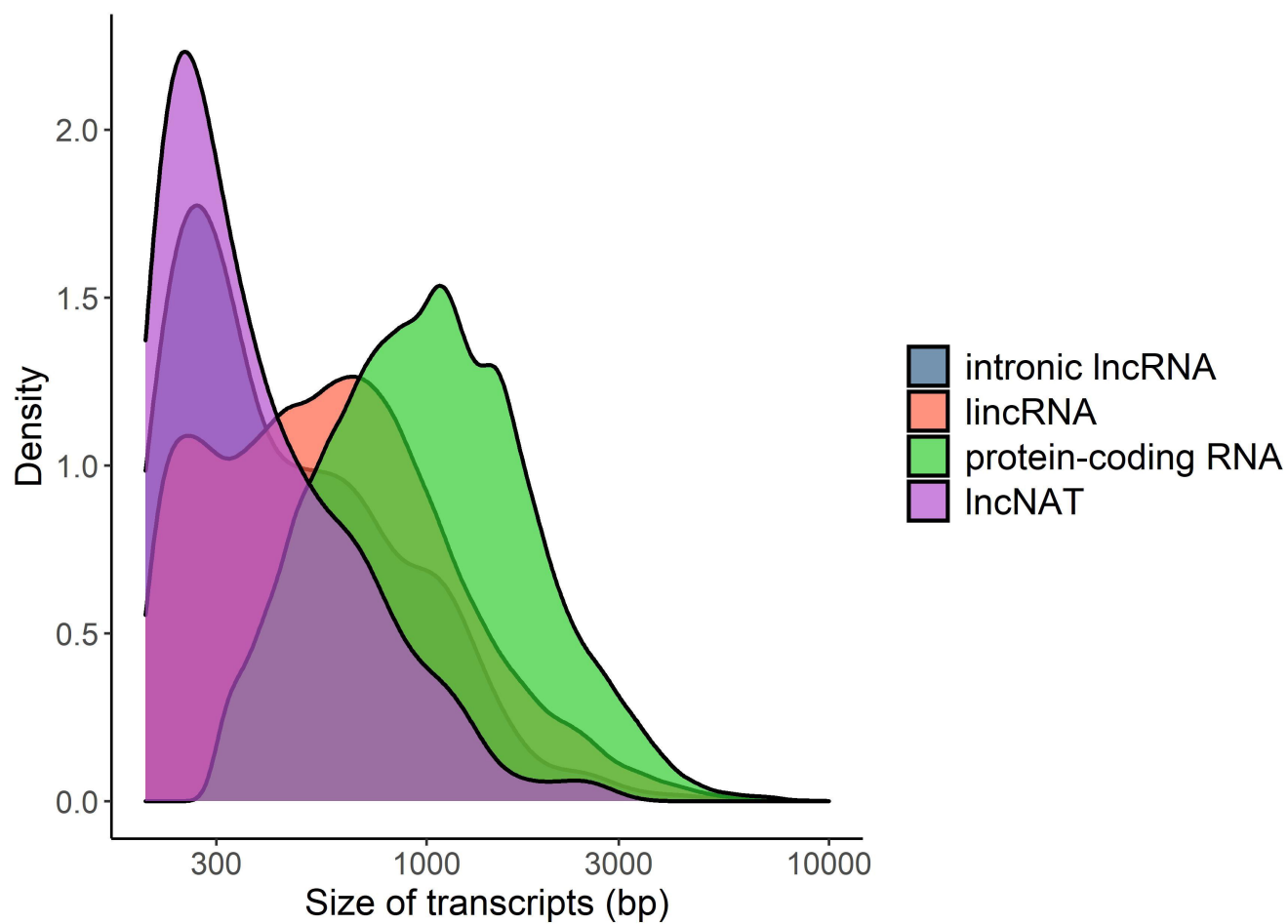
- 1 RNA transcripts. *Nucleic Acids Research* **43**: e78.
- 2 **Therneau TM. 2020.** Survival Analysis. R package survival version 3.2-7.
- 3 **Tian J, Song Y, Yang X, et al. 2016.** Population genomic analysis of gibberellin-
4 responsive long non-coding RNAs in *Populus*. *Journal of Experimental Botany* **67**:
5 2467–2482.
- 6 **Tripathi R, Chakraborty P, Varadwaj PK. 2017.** Unraveling long non-coding RNAs
7 through analysis of high-throughput RNA-sequencing data. *Non-coding RNA Research*
8 **2**: 111–118.
- 9 **Visser EA, Wegrzyn JL, Myburg AA, Naidoo S. 2018.** Defence transcriptome
10 assembly and pathogenesis related gene family analysis in *Pinus tecunumanii* (low
11 elevation). *BMC Genomics* **19**: 632.
- 12 **Visser EA, Wegrzyn JL, Steenkamp ET, Myburg AA, Naidoo S. 2019.** Dual RNA-
13 seq analysis of the pine-*Fusarium circinatum* interaction in resistant (*Pinus*
14 *tecunumanii*) and susceptible (*Pinus patula*) hosts. *Microorganisms* **7**: 7–9.
- 15 **Visser EA, Wegrzyn JL, Steenkamp ET, Myburg AA, Naidoo S. 2015.** Combined *de*
16 *novo* and genome guided assembly and annotation of the *Pinus patula* juvenile shoot
17 transcriptome. *BMC Genomics* **16**: 1057.
- 18 **Wang KC, Chang HY. 2011.** Molecular Mechanisms of Long Noncoding RNAs.
19 *Molecular Cell* **43**: 904–914.
- 20 **Wang Zupeng, Liu Y, Li L, et al. 2017.** Whole transcriptome sequencing of
21 *Pseudomonas syringae* pv. *actinidiae*-infected kiwifruit plants reveals species-specific
22 interaction between long non-coding RNA and coding genes. *Scientific Reports* **7**: 1–15.
- 23 **Wang Y, Luo X, Sun F, et al. 2018.** Overexpressing lncRNA LAIR increases grain

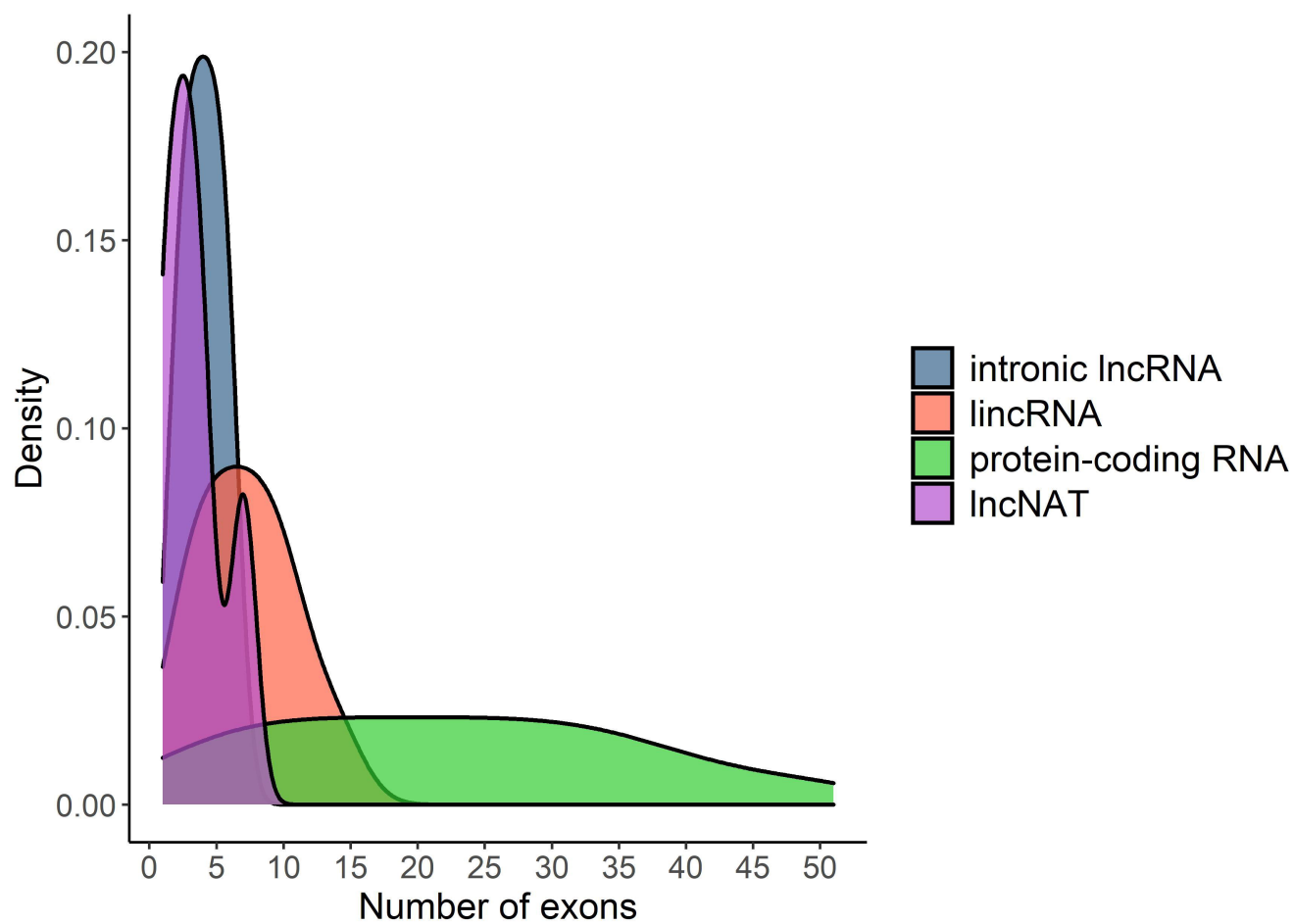
- 1 yield and regulates neighbouring gene cluster expression in rice. *Nature*
2 *Communications* **9**: 1–9.
- 3 **Wang M, Yuan D, Tu L, et al. 2015.** Long noncoding RNAs and their proposed
4 functions in fibre development of cotton (*Gossypium* spp.). *New Phytologist* **207**: 1181–
5 1197.
- 6 **Wang Zhe, Zhai X, Cao Y, Dong Y, Fan G. 2017.** Long non-coding RNAs responsive
7 to Witches' Broom disease in *Paulownia tomentosa*. *Forests* **8**: 348.
- 8 **Wegrzyn JL, Lee JM, Tearse BR, Neale DB. 2008.** TreeGenes: A Forest Tree
9 Genome Database. *International Journal of Plant Genomics* **2008**: 1–7.
- 10 **Wingfield MJ, Hammerbacher A, Ganley RJ, et al. 2008.** Pitch canker caused by
11 *Fusarium circinatum* - A growing threat to pine plantations and forests worldwide.
12 *Australasian Plant Pathology* **37**: 319–334.
- 13 **Wucher V, Legeai F, Hédan B, et al. 2017.** FEELnc: A tool for long non-coding RNA
14 annotation and its application to the dog transcriptome. *Nucleic Acids Research* **45**: 57.
- 15 **Young MD, Wakefield MJ, Smyth GK, Oshlack A. 2010.** Gene ontology analysis for
16 RNA-seq: accounting for selection bias. *Genome Biology* **11**: 14.
- 17 **Yu X, Feng B, He P, Shan L. 2017.** From Chaos to Harmony: Responses and
18 Signaling upon Microbial Pattern Recognition. *Annual Review of Phytopathology* **55**:
19 109–137.
- 20 **Yu G, Wang LG, Han Y, He QY. 2012.** ClusterProfiler: An R package for comparing
21 biological themes among gene clusters. *OMICS A Journal of Integrative Biology* **16**:
22 284–287.
- 23 **Yu Y, Zhang Y, Chen X, Chen Y. 2019.** Plant noncoding RNAs: Hidden players in

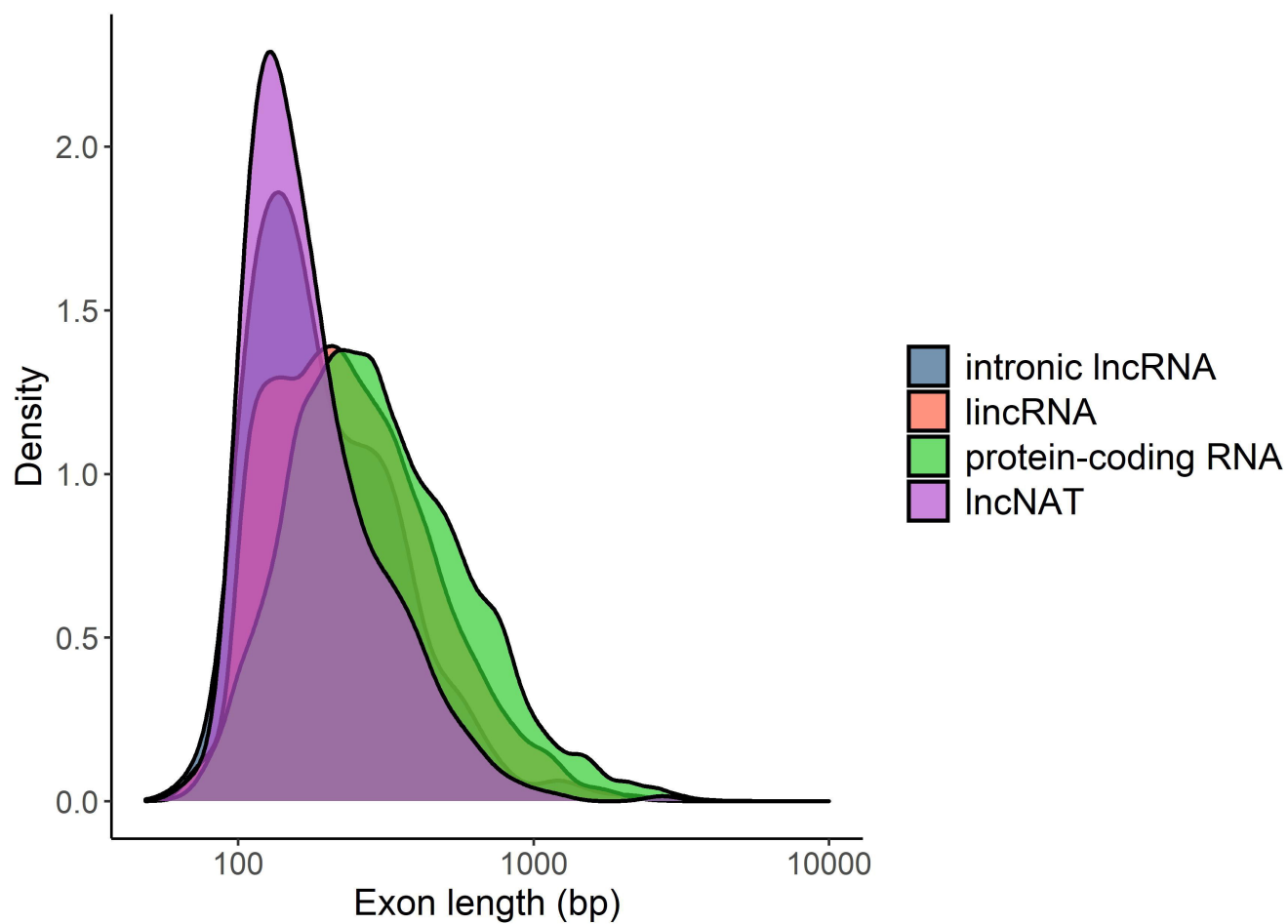
- 1 development and stress responses. *Annual Review of Cell and Developmental Biology*
2 **35**: 407–431.
- 3 **Yu Y, Zhou YF, Feng YZ, et al. 2020.** Transcriptional landscape of pathogen-
4 responsive lncRNAs in rice unveils the role of ALEX1 in jasmonate pathway and
5 disease resistance. *Plant Biotechnology Journal* **18**: 679–690.
- 6 **Zamora-Ballesteros C, Diez JJ, Martín-García J, et al. 2019.** Pine Pitch Canker
7 (PPC): Pathways of Pathogen Spread and Preventive Measures. *Forests* **10**: 1158.
- 8 **Zamora-Ballesteros C, Pinto G, Amaral J, et al. 2021.** Dual RNA-Sequencing
9 Analysis of Resistant (*Pinus pinea*) and Susceptible (*Pinus radiata*) Hosts during
10 *Fusarium circinatum* Challenge. *International Journal of Molecular Sciences* **22**: 5231.
- 11 **Zaynab M, Fatima M, Abbas S, et al. 2018.** Role of secondary metabolites in plant
12 defense against pathogens. *Microbial Pathogenesis* **124**: 198–202.
- 13 **Zhang L, Wang M, Li N, et al. 2018.** Long noncoding RNAs involve in resistance to
14 *Verticillium dahliae*, a fungal disease in cotton. *Plant Biotechnology Journal* **16**: 1172–
15 1185.
- 16 **Zhao Q, Guo HW. 2011.** Paradigms and paradox in the ethylene signaling pathway and
17 interaction network. *Molecular Plant* **4**: 626–634.
- 18 **Zhu Q-H, Stephen S, Taylor J, Helliwell CA, Wang M-B. 2014.** Long noncoding
19 RNAs responsive to *Fusarium oxysporum* infection in *Arabidopsis thaliana*. *New*
20 *Phytologist* **201**: 574–584.

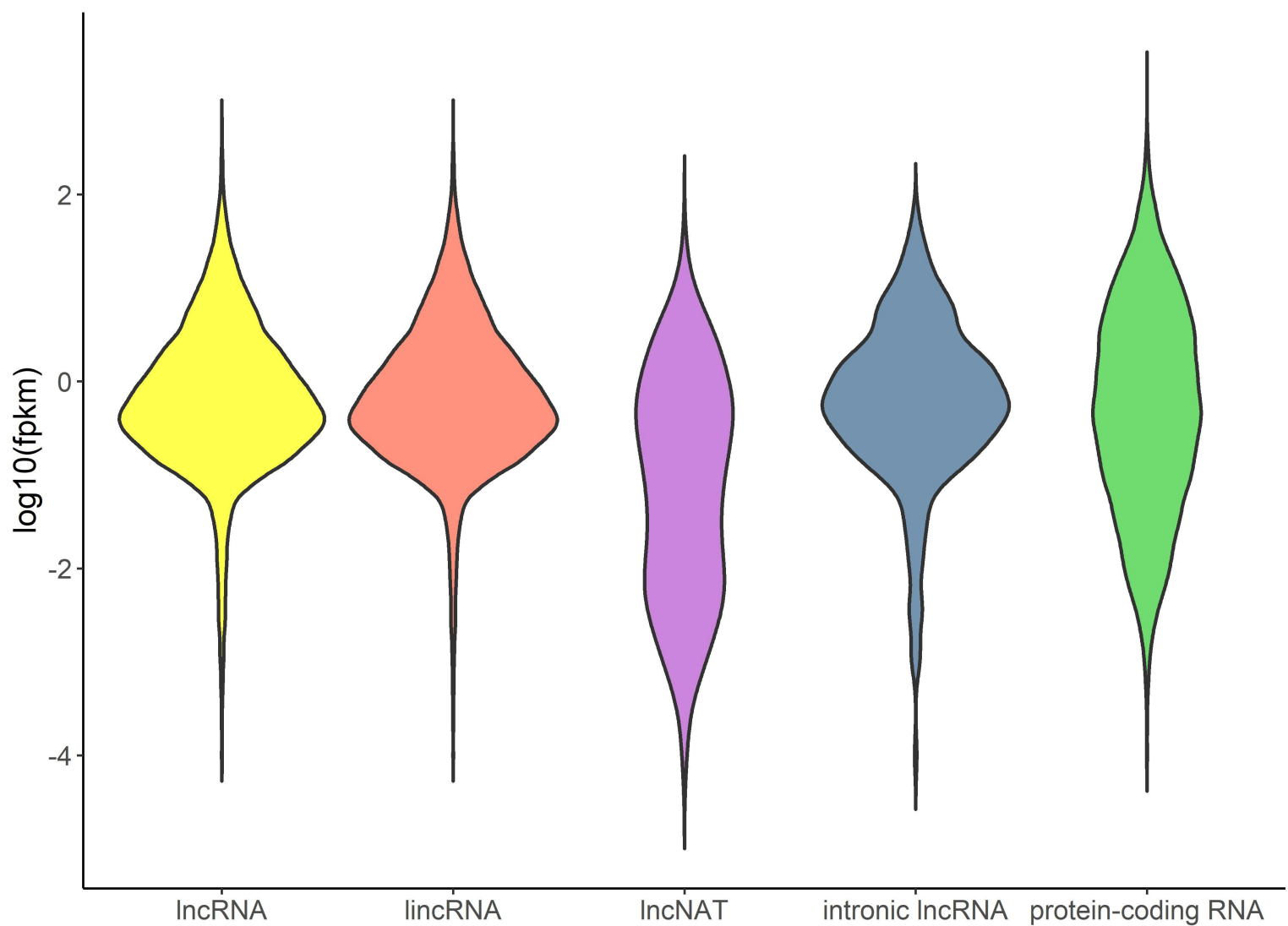


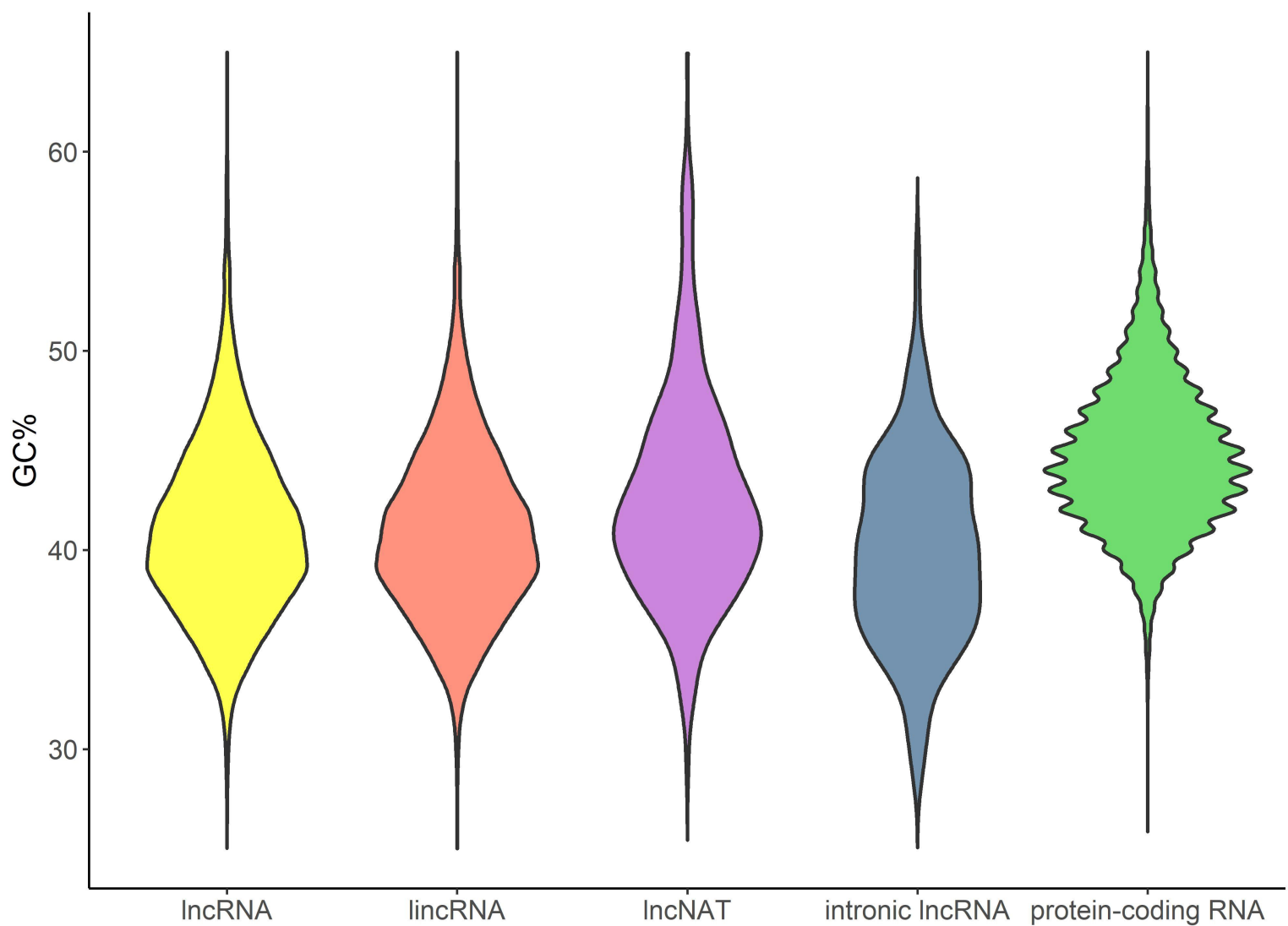












Color Key and Histogram

